Total Synthesis and Biological Evaluation of a Series of Macrocyclic Hybrids and Analogues of the Antimitotic Natural Products Dictyostatin, Discodermolide, and Taxol

ARTICLE *in* CHEMISTRY - AN ASIAN JOURNAL · FEBRUARY 2011

Impact Factor: 4.59 · DOI: 10.1002/asia.201000541 · Source: PubMed

5 AUTHORS, INCLUDING:

Esther Guzman
Florida Atlantic University
33 PUBLICATIONS **398** CITATIONS
SEE PROFILE

Amy E Wright
Florida Atlantic University
94 PUBLICATIONS **2,165** CITATIONS
SEE PROFILE

Published in final edited form as:
Chem Asian J. 2011 February 1; 6(2): 459–473. doi:10.1002/asia.201000541.

Total Synthesis and Biological Evaluation of a Series of Macrocyclic Hybrids and Analogues of the Antimitotic Natural Products Dictyostatin, Discodermolide and Taxol

Ian Paterson[*,a], **Guy J. Naylor**[a], **Nicola M. Gardner**[a], **Ester Guzmán**[b], and **Amy E. Wright**[b]
[a]University Chemical Laboratory, Lensfield Road, Cambridge, CB2 1EW, UK

[b]Harbor Branch Oceanographic Institution at Florida Atlantic University, 5600 US 1 North, Fort Pierce, FL 34946, USA

Abstract

The design, synthesis and biological evaluation of a series of hybrids and analogues of the microtubule-stabilising anticancer agents dictyostatin, discodermolide and taxol is described. A 22-membered macrolide scaffold was prepared by adapting earlier synthetic routes directed towards dictyostatin and discodermolide, taking advantage of the distinctive structural and stereochemical similarities between these two polyketide-derived marine natural products. Initial endeavours towards accessing novel discodermolide/dictyostatin hybrids led to the adoption of a late-stage diversification strategy and the construction of a small library of methyl ether derivatives, along with the first triple hybrids bearing the side chain of taxol or taxotere attached through an ester linkage. Following biological assays of the antiproliferative activity of these compounds in a series of human cancer cell lines, including the taxol-resistant NCI/ADR-Res cell line, the results allowed the proposal of various structure-activity relationships. This led to the identification of a potent macrocyclic discodermolide/dictyostatin hybrid **12** and its C9 methoxy derivative **38**, accessible by an efficient total synthesis and having a similar biological profile to dictyostatin.

Keywords

natural products; macrolides; total synthesis; designed analogues; hybrids; cytotoxic; tubulin

Introduction

Cancer is one of the leading causes of mortality in the developed world and its increasing prevalence highlights the compelling need to generate new and more effective therapies. One of the most promising avenues of anti-cancer research is the study of natural products that attenuate cancer cell growth by acting as inhibitors of cellular microtubules.1 These compounds fall into two distinct groups: those that inhibit the assembly of tubulin heterodimers into microtubule polymers and those which stabilize microtubules.[2] These latter microtubule-stabilising agents (MSA) impede the depolymerization of microtubules into their dimeric αβ-tubulin subunits, thereby preventing mitosis due to stabilization of the

Fax: (+44)1223-336362, ip100@cam.ac.uk, Homepage: http://www-paterson.ch.cam.ac.uk/.
[*]Prof. Dr. I. Paterson, G. J. Naylor, Dr. N. M. Gardner, Dr. E. Guzmán, and Dr. A. E. Wright.

Dedicated to Professor Eiichi Nakamura on the occasion of his 60th birthday.

Supporting information for this article is available on the WWW under http://dx.doi.org/ or from the author.

mitotic spindle, leading to a block in the cell cycle at the G_2/M phase and cell death *via* apoptosis.

The diterpenoid compound taxol (paclitaxel, **1**, Fig. 1) was first isolated in 1962 from the Pacific Yew tree *Taxus Brevifolia* and was the first microtubule-stabilising agent to be discovered.[3] However, its biological mode of action remained unresolved for nearly two decades until Horwitz and co-workers revealed their seminal findings in 1979.[4] Since gaining *FDA* approval in 1992, Taxol® and subsequently its semi-synthetic analogue Taxotere® (docetaxel, **2**)[5] have experienced widespread clinical use in a range of oncology treatments including breast, ovarian and lung cancers. Although the taxane class of cytotoxic drugs have great utility as chemotherapeutic agents, they suffer from low aqueous solubility and a tendency for drug resistance to develop in patients, further underlining the continued need for the identification of new microtubule-stabilising agents.[6] This has led to the search for structurally novel natural product scaffolds that share the same mode of action as the taxanes but have superior efficacy to overcome drug resistance. A major breakthrough was the discovery of the epothilones and the subsequent development of the semi-synthetic lactam derivative Ixempra® as a clinically important anticancer drug.[7]

Discodermolide[8] (**3**) and dictyostatin[9] (**4**) are both marine sponge-derived polyketides which share the same microtubule-stabilising mode of action as taxol. Significantly, they are poor substrates for the P-glycoprotein efflux pump and hence are able to maintain their antiproliferative ability against taxol-resistant cancer cell lines. Both discodermolide and dictyostatin are thought to bind at either the luminal taxoid binding site on β-tubulin or the recently discovered exterior pore site.[10] Assays also found the two drugs to have appreciably higher binding affinities than taxol; indeed discodermolide has the highest affinity of any known MSA,[11] and was also shown to have a synergistic relationship with taxol,[12] supporting their potential use together in combination therapies. Such promising anticancer properties have made discodermolide the focus of intensive synthetic and biological interest, [13] culminating in the remarkable total synthesis of >60 g of this architecturally complex natural product for use in a Phase I clinical trial by Novartis,[14] where unfortunately pulmonary toxicity issues arose.[15]

Key to understanding the cellular behaviour of these compounds, and crucial for the design of simplified and more potent analogues, is the determination of their bioactive 3D conformations and their orientations within the taxoid binding site. To this end, numerous, and often conflicting, binding models have been postulated for taxol. Of the proposals, two preferred structures are “T-Taxol”, as proposed by Snyder and co-workers,[16,17] and “REDOR-Taxol” which was put forward by Ojima and co-workers.[18] Though broadly in agreement, a vigorous debate has since ensued as to the relative merits of these two viewpoints.[17,19]

As a lead structure for the generation of novel chemotherapeutic agents, discodermolide has also been a focus of extensive studies to elucidate the details of its binding interactions with β-tubulin and microtubules. The solid state structure of discodermolide was resolved *via* X-ray crystallography to be “hairpin-like”, where the compound adopts a preorganized U-shaped conformation.[8a] The relative importance of this 3D structure for solution and protein-bound environments has been hotly contested. However, a combination of NMR techniques and molecular modelling increasingly indicate that the hairpin structure is conserved across all three of these environments (Fig. 2). [20,21] This distinctive conformational preorganization in discodermolide can be largely traced to the highly substituted propionate-derived backbone, with the mimimization of *syn-pentane* steric interactions and A(1,3)-strain about the $\Delta^{8,9}$, and $\Delta 13,14$, alkenes.[22]

With respect to the orientation of the ligand within the protein binding pocket, there is still some debate. Canales *et al*. used the AutoDock program to analyse the interactions of bioactive, conformationally-locked discodermolide with β-tubulin, finding that the compound sat exactly in the luminal taxoid binding site.[20] Snyder and co-workers re-examined this calculation using the same discodermolide hairpin coordinates, but employing three different docking programs.[23] They identified two distinct poses within the taxoid binding site, one of which was a precise match for Canales' binding model.

With intriguing structural similarities to discodermolide, the 22-membered macrolide dictyostatin has recently emerged as a new MSA with promising anticancer properties, and has been the focus of extensive synthetic and biological studies.[24] To date, only one group has attempted to propose a model of dictyostatin binding. In an ambitious paper, Canales *et al*. reported a unified binding model for taxol, discodermolide and dictyostatin.[20] As previously described, the solution and tubulin-bound conformation of discodermolide were determined *via* NMR techniques and found to be strikingly similar. However, the same methods when applied to dictyostatin revealed a profound difference in these structures, implying that a far higher degree of conformational selection is required during the binding event. Significantly, the bound conformer of dictyostatin was discovered to closely resemble bound discodermolide, suggesting that the two compounds could potentially share the majority of their interactions with common amino acid residues of the protein. This supposition was further supported by the results of docking these bioactive conformations onto tubulin with AutoDock. Dictyostatin was found to occupy the taxoid site in a closely correlated pose to discodermolide, as can been seen in the overlaid image of the two ligands bound to β-tubulin (Fig. 3).

Superimposition of all three MSAs at the taxoid site, reveals discodermolide and dictyostatin to not fully occupy the taxol binding pocket. The two polyketides sit in the same region as the polycyclic baccatin core of taxol, but the C13 side chain of taxol extends into a cleft of the binding site which is not exploited by either discodermolide or dictyostatin. We proposed to use these tubulin binding models of Canales *et al*. as the basis for the rational design of a discodermolide-dictyostatin double hybrid and, more speculatively, for a series of triple hybrids incorporating the taxol side chain.

Results and Discussion

Synthesis of Hybrids of Dictostatin, Discodermolide and Taxol

Prior to Canales *et al*. reporting their findings, as part of our on-going efforts to generate highly potent analogues of dictyostatin,[24h] our group embarked on a synthesis of a discodermolide/dictyostatin hybrid.[25] Initial investigations were stimulated by their identical biological modes of action and the striking structural similarities between discodermolide and dictyostatin when the two linear carbon backbones are compared (Fig. 4). Encouraging initial findings on some simplified discodermolide/dictyostatin hybrids had been also been reported by the Curran group[24a] before the full configuration of dictyostatin had been determined.[9c]

At the outset, in-house molecular modelling had indicated that the lowest energy conformer of discodermolide in water possessed the same hairpin geometry seen in the X-ray crystal structure and overlaid closely with the lowest energy structure of the dictyostatin macrolide. This led to the design of the 22-membered macrolide structure **5** (Scheme 1), incorporating the full C2–C24 linear sequence of discodermolide and the (*Z*)-enoate of dictyostatin.[25] It was hypothesized that restricting the open chain structure of discodermolide into a macrocyclic motif, inspired by dictyostatin, would help in reducing any conformational selection that would be required for tubulin binding.

The retrosynthetic analysis for this initial hybrid structure was heavily influenced by our group's previous endeavours towards achieving a practical and highly stereoselective synthesis of discodermolide, along with having access to stocks of key advanced intermediates.[26] Following our second generation total synthesis of discodermolide, a boron-mediated aldol reaction of ketone **6** and aldehyde **7** would be the centrepiece of this synthesis of macrocyclic analogue **5**, followed by a Yamaguchi macrolactonization[27] to close the 22-membered macrolactone.

Aldehyde **7** was conveniently accessed *via* a straightforward synthetic sequence from known diol **8** which incorporates the required stereotriad configuration (Scheme 2).26b,c The more stereochemically elaborate ketone **6** was generated from *bis*-PMB ether **9**, an advanced C13– C24 intermediate employed in our earlier discodermolide synthesis,26a,b *via* an efficient 3-step sequence to install the *Z*-enone.[26d] Selective removal of the primary PMB ether was achieved on treatment of **9** with BCl_3·DMS,[28] followed by TEMPO/$PhI(OAc)_2$ oxidation[29] of the resulting alcohol to the aldehyde and Still-Gennari olefination[30] to afford **6** (10:1 *Z*/*E*). The two coupling partners were now subjected to the pivotal aldol reaction. Enolization of methyl ketone **6** with *c*-Hex_2BCl and Et_3N in ether at 0 °C led to the formation of the required boron enolate after 1 h. Subsequent addition of an ethereal solution of aldehyde **7** at −78 °C and stirring for 15 min resulted in complete consuption of the limiting aldehyde partner to give aldol adduct **10** (48%), with essentially complete diastereoselectivity at C7 (>95 : 5 dr). The high level of stereocontrol with an anti-Felkin-Anh bias in this complex aldol coupling can be rationalized by invoking the preferred cyclic transition state **TS 1** which is consistent with our earlier work on exploiting 1,6-stereoinduction from structurally similar (*Z*)-enones in the context of our second generation total synthesis of discodermolide.26c,d

Having formed the key C7-C8 bond, the complete carbon backbone of the hybrid was now in place. The endgame strategy commenced with setting the final C9 stereocentre *via* CBS reduction[31] of the enone, which afforded the desired 1,3-*anti* diol with reasonable stereoselectivity (75 : 25 dr, Scheme 3). Acetonide protection and oxidative cleavage of both PMB ethers mediated by DDQ yielded the primary alcohol **11** (56% over three steps). A two-step oxidation sequence rapidly generated the *seco-acid*, which underwent macrolactonization under modified Yamaguchi conditions24c,[32] (63%). Finally, global deprotection (3N HCl, MeOH, x%) afforded the targeted discodermolide-dictyostatin hybrid **5**. Following HPLC purification, this initially designed hybrid construct was submitted to biological evaluation along with other synthetic analogues, as described later.

When planning our second generation hybrid,[33] we had the additional benefit of being able to refer to the binding models proposed by Canales *et al*.[20] The structural similarities between discodermolide and dictyostatin coincide with the regions of greatest overlap, with the largest spatial discrepancies corresponding to the δ-lactone and dienoate functionalities. In designing the second generation double hybrid **12**, we chose to furnish the regions of closest overlap (C8 to C26) with the discodermolide substitution pattern, while the region of greatest difference (C1 to C7) would be entirely dictyostatin-derived (Scheme 4). It was anticipated that the superior assembly-inducing ability of dictyostatin[11] could, in part, be aided by the dienoate, and this might be reflected in enhanced potency of this structurally more dictyostatin-like hybrid compared to **5**.

Our retrosynthetic analysis was also altered with respect to the initial hybrid **5**, with a cross-coupling-macrolactonization strategy preceded by an elaborate Still-Gennari olefination to unite the northern discodermolide hemisphere with the southern dictyostatin fragment. This would employ the highly functionalized β-ketophosphonate **14**, an intermediate initially developed for our recently reported second generation total synthesis of dictyostatin.[34]

Employing the same optimized conditions as utilized for dictyostatin (K_2CO_3, 18-crown-6, PhMe/HMPA, 0 °C), the known aldehyde **13**[26a] and β-ketophosphonate **14** successfully underwent an olefination reaction on gram scale to set the (*Z*)-alkene in 67% isolated yield with 6.9:1 (*Z:E*) selectivity (Scheme 5). With enone **16** in hand, the remainder of the carbon backbone was rapidly assembled. As with the previous hybrid **5**, the most successful method for reducing the enone was under CBS conditions (>95 : 5 dr), which was carried out subsequent to cleavage of the β-PMB ether (DDQ, 88%) in order to achieve synthetically useful levels of selectivity. The success of this approach was in marked contrast to the poor conversion and low selectivity encountered under Evans-Saksena conditions.[35]

Acetonide protection proceeded smoothly (86% over two steps), before a copper-mediated Stille-Liebeskind cross-coupling[36] between vinyl iodide **17** and stannane **15** completed the carbon backbone by installing the (2*Z*,4*E*)-dienoate. Macrolactonization under modified Yamaguchi conditions smoothly afforded the fully protected macrocycle, which was then deprotected (3N HCl, MeOH) to provide hybrid **12** (72%), with minimal translactonization onto the C19 hydroxyl.

To further investigate the pharmacophore of this hybrid, and in particular the contribution of the C7,C9-diol, **12** was then treated with 2,2-dimethoxypropane and catalytic PPTS to reintroduce the acetonide into analogue **18**.

Taking inspiration from our earlier dictyostatin analogue work,[24e] the utility of the minor (*E*)-enone isomer obtained from the noteworthy Still-Gennari olefination giving **16** was explored. This late-stage intermediate could undergo selective conjugate reduction of the (10*E*)-enone and then be elaborated to a dihydro-analogue of hybrid **12**. Semi-synthetic removal of the analogous olefin (along with several others) *via* catalytic hydrogenation of discodermolide to generate the reduced derivatives **19–21** had provided useful SAR insights (Fig. 5).[37] Furthermore, the 10,11-dihydro analogue **22** of dictyostatin was found to maintain its antiproliferative potency against most cancer cell lines, with only moderate increases in IC_{50} values. There was a marked reduction in cytotoxicity against the taxol resistant NCI/ADR-Res cell line however, implicating this olefin in playing a crucial role in avoiding an undesired protein residue contact with any mutations on β-tubulin, or in reducing its affinity for the P-glycoprotein efflux pump mechanism.

Analogue **23** would differ from the original 10,11-dihydrodictyostatin **22** by the additional methyl bearing stereocentre at C18 and the incorporation of a (*Z*)-trisubstituted olefin at C15-C16, with collateral loss of the C16 stereocentre. This additional hybrid was viewed as offering a useful contribution to the SAR model for both dictyostatin and discodermolide.

Closely emulating our earlier work, conjugate reduction of enone **24** with freshly prepared Stryker's reagent[38] ($[Ph_3PCuH]_6$) provided the saturated ketone which was then submitted to DDQ-mediated PMB deprotection (87%) to give diol **25** (Scheme 6). Whereas reduction of the analogous unsaturated β-hydroxy ketone precursor to hybrid **12** with (*R*)-CBS and BH_3·THF proved to be almost completely diastereoselective, on this substrate no useful selectivity was observed. Fortunately, Evans-Saksena conditions ($Me_4NBH(OAc)_3$, MeCN / THF, 2:1) also manifested the opposite behaviour with **25** and now effected reduction with excellent levels of diastereoselectivity in favour of the desired 1,3-*anti* diol **26** (>95 : 5 dr, 55% yield, 91% brsm). It is thought that the previous CBS reduction experienced a degree of matched substrate, as well as reagent stereocontrol and saturation of the $\Delta^{10,11}$ olefin had sufficiently altered the conformation of the reactant to remove this substrate bias which may also have destabilized the normally preferred Evans-Saksena transition state.39

With the 1,3-*anti* diol **26** in hand, the synthesis of analogue **23** was completed in four steps (58%), following the route taken earlier for hybrid **12**. The only slight modification being a

reduction in the number of equivalents of DMAP in the macrocyclization step to minimize isomerism of the (4*E*,2*Z*)-dienoate to the more thermodynamically favourable (4*E*,2*E*) configuration.[40]

As alluded to above, the unified binding model espoused by Canales *et al*. proposes that discodermolide and dictyostatin are located in the area of the binding site occupied by the baccatin core of taxol (Fig. 3). In addition, the C13 side chain of taxol occupies a further region of the pocket that is not taken advantage of by either of the polyketide structures. However, the C7 and C9 hydroxyls on dictyostatin are orientated to point into this unexploited pocket, and presumably this would also be true for double hybrid **12**. By appending the taxol or taxotere side chain onto either of these hydroxyls, it was hypothesized that additional binding interactions could be gleaned and in doing so (to the best of our knowledge) generate the first triple hybrids.[41]

Taking advantage of fully protected macrolactone **27**, an advanced intermediate in the synthesis of hybrid **12**, a late-stage diversification strategy was pursued. Acetonide deprotection was affected with PPTS, MeOH/DCM (1:1) to yield the 1,3-diol **28** which would be the substrate for esterification (Scheme 7). Attachment of the side chains was achieved by following a modification of the original protocol developed to introduce the taxane side chain onto the C13 hydroxyl of baccatin III.[42] Accordingly, deprotonation of **28** with NaHMDS followed by treatment with β-lactam **29** (taxol side chain, R = Ph) or **30** (taxotere side chain, R = O^{t}Bu)[43] provided an inseparable mixture of regioisomeric esters. The ratio of C7 to C9 ester was found to be temperature dependent; for lactam **29** (R = Ph), the C9-coupled product dominated at 0 °C (2 : 1) while at lower temperatures, this selectivity was overturned and surprisingly the more sterically hindered C7 hydroxy was the favoured reaction site (3:1). This mixture of esters was then deprotected under mild conditions (HF·py, pyridine) to yield the desired triple hybrids **31–34** which were separated by careful HPLC purification.

Attempted NMR characterization of these hybrids using deuterated DMSO and methanol brought to light several unexpected stability issues. Irrespective of the hybrid studied, dissolving in d6-DMSO resulted in regiomerically pure hybrid undergoing tranesterification to produce an approximate 2:1 mixture of C9 to C7 esters. Upon heating, the bias towards the C9 regioisomer was further reinforced, presumably due to the more benign steric environment of this position. This result was especially notable as DMSO is commonly used as a solvent in biological assays, meaning any results could not be assumed to be for the pure compound. Intriguingly, after 72 h in methanol solution the side chains were found to be labile, reforming the original double hybrid **12** and the corresponding methyl ester derived from the taxol or taxotere side chain.

Drawing on findings from previous dictyostatin analogues prepared in the group, our attention was drawn to the highly potent 9-methoxydictyostatin derivative.[24c] In emulating this work, it was anticipated that by capping the C7 or C9 free hydroxyl as the methyl ether, we could prevent the undesired transesterification processes witnessed in DMSO and methanol, without significantly altering the biological profile of the compounds.

Satisfyingly, treatment of diol **28** with Meerwein's salt and Proton Sponge® was found to be highly regioselective (~30 : 1) for the more nucleophilic C9 allylic alcohol (Scheme 8). The reaction time was found to be critical to preventing formation of the *bis*-methyl ether **35**, typically the reaction had to be halted early and unreacted starting material recovered. However, sufficient quantities of **35** were isolated from initial reactions to be advanced to the C7,C9-dimethoxy derivative **36**. With the selectively methylated compound **37** in hand, deprotection with HF·py gave the novel C9 methoxy analogue **38**, whereas esterification

with β-lactam **29** or **30** followed by subsequent deprotection gave esterified triple hybrids **39** and **40** (78% and 91% yield over two steps respectively).

A less direct approach would be necessary to access the corresponding C7 methoxy compounds. Continuing our policy of late-stage diversification, the C9 hydroxy would first be selectively protected followed by C7–OH methylation and then C9 deprotection. This was achieved by treatment of 1,3-diol **28** with TESOTf and 2,6-lutidine in 71% yield. Although this reaction proceeded in good regioselectivity (5 :1 at −78 °C, further enhanced to >10:1 at – 100 °C), *bis*-silylation was also surprisingly facile (Scheme 9). Despite using only 1.1 equiv. of TESOTf, 17% of **41** was generated as well as recovering 13% of unreacted starting material. Consequently, the *bis*-TES material was recycled back to diol **28** *via* a high-yielding PPTS, MeOH-DCM deprotection (96%) to minimize loss of material.

Reaction of mono-TES compound **42** with Meerwein's salt to cap the C7 free hydroxyl was then followed by selective cleavage of the TES group (99%). At this stage, global deprotection led to the C7 methoxy analogue **44**, whilst treatment with NaHMDS and β-lactam **29** or **30** and subsequent deprotection gave *O*-methylated triple hybrids **45** and **46** (65% and 77% yield over two steps respectively).

Evaluation of the methyl ether triple hybrids **39, 40, 45** and **46** demonstrated the successful elimination of all chemical stability issues. All compounds were found to be stable in DMSO at ambient temperature for several weeks, and the side chains were now unaffected by exposure to methanol. These results indicate that the neighbouring free hydroxyl plays a decisive role in the transesterification of hybrids **31–34**.

Biological Evaluation

All of the prepared compounds were submitted to in *vitro* biological assays against at least two human cancer cell lines and their activities compared to taxol (**1**), discodermolide (**3**) and dictyostatin (**4**). The participating cell lines consisted of the AsPC-1 (pancreatic), DLD-1 (colon), PANC-1 (pancreatic) and NCI/ADR-Res (taxol-resistant ovarian), and all IC_{50} values quoted are the average from a minimum of three experiments.

The most potent of the new compounds were the second-generation double hybrid **12**, and its close structural derivative the 9-methoxy analogue **38**, both displaying low nanomolar cytotoxicities in taxol-sensitive and taxol-resistant cell lines. The moderate cytotoxicity of the macrocyclic discodermolide hybrid **5** indicates that it is a much poorer antiproliferative agent than either of the two parent natural products, though it was still able to induce a G_2/M block in cell cycle analysis assays. The structural differences between hybrids **5** and **12** (removal of substitution at C4 and C5 and replacement with an (*E*)-alkene) have a profound effect on cell growth inhibition capabilities. These alterations could allow **5** to access a disparate lowest energy conformation that bears little similarity to the bioactive conformer, or it could be allowing unfavourable binding interaction to occur at the taxoid site. The satisfying biological results obtained for dictyostatin/discodermolide hybrid **12** (IC_{50} values intermediate between that measured for discodermolide and dictyostatin) acted as an incentive for its use as a lead compound for the generation of this diverse group of analogues and further hybrids. In analysing the results for these compounds some potential SAR trends have been identified.

The 10,11-dihydro analogue **23** was found to be at least one order of magnitude less active than its unsaturated equivalent **12**. This loss in activity was especially noticeable in the taxol-resistant NCI/ADR-Res cell line and broadly is in agreement with the behaviour of 10,11-dihydro dictyostatin **22**.[24e] The results for acetonide **18** are more enlightening when contrasted with those for 7,9-dimethoxy hybrid **36**. Analogue **18** has a relatively poor

biological profile and does not cause an accumulation of cells at the G_2/M block, whereas **36** is approximately equipotent with discodermolide. This suggests that neither of the C7,C9 hydroxyls are involved in stabilising hydrogen bonding interactions, and are probably not located in a sterically congested part of the binding site. However, the conformational rigidity imparted by the acetonide has a highly detrimental effect, potentially perturbing the bioactive conformation.

All of the triple hybrids **31–34** proved to be less cytotoxic than the parent double hybrid **12**, demonstrating that the addition of the side chains did not lead to improved tubulin binding ability. Closer inspection also revealed a marked reduction in IC_{50} values for these hybrids (including the *O*-methylated derivatives), when comparing the PANC-1 results with those for NCI/ADR-Res. The presence of a taxane side chain appears to introduce limitations associated with the taxoid family. The values for the 7- and 9-taxotere hybrids **32** and **34** for both cell lines are surprisingly similar, and when taking into account the standard deviations, are virtually indistinguishable. This implies that the test was done on a mixture of regioisomers, the expected tranesterification having arisen in the DMSO stock solution used to dissolve the compounds in preparation for the assays. For the corresponding taxol hybrids **31** and **33**, the tranesterification does not seem to have occurred to the same extent as evidenced by the dissimilarity of their IC_{50} values. Comparing the different side chains, taxotere hybrids **32, 34, 40** and **46** fared better in the pancreatic cell line, while their taxol counterparts **31, 33, 39** and **45** performed more effectively in the taxol-resistant ovarian line.

Introduction of the methoxy functionality at the C7 position had a slightly negative impact, in particular for the NCI/ADR-Res cell line (interestingly, the dimethoxy congener **36** was more potent than **44** in this cell line). However, the 9-methoxy double hybrid **38** proved to be the most potent of all the synthesized compounds (with IC_{50} = 8.2 nM in the resistant NCI/ADR-Res cell line)), approaching the IC_{50} values of dictyostatin itself. Furthermore, the 9-methoxy triple hybrids **39** and **40** were noticeably more active than the 7-methoxy hybrids **45** and **46**. In the cell cycle assays, C7-methoxy **44** caused 72% of the cell population to accumulate at the G_2/M block (PANC-1 treated with 100 nM of compound), while the C9-methoxy could manage an impressive 93%, matched exactly by the C7,C9-dimethoxy (also 93%).

Conclusions

In carrying out this work, we have successfully designed and synthesized a series of novel hybrids of the antimitotic natural products discodermolide, dictyostatin and taxol which share a common microtubule stabilising mode of action and tubulin binding site. The biological profile of the majority of these compounds is highly encouraging, with the dictyostatin/discodermolide hybrid **12** and its 9-methoxy derivative **38** especially worthy of note. These two compounds are now the focus of efforts to produce a quantity sufficient for *in vivo* testing. The triple hybrids, though displaying pleasing levels of cytotoxicity, did not lead to an increase in activity relative to the double hybrid **12** (contrast this with baccatin III and taxol). A number of factors could have contributed to this, including the increased polarity of the compounds now making them less cell permeable. The SAR trends revealed for these compounds will prove useful in the design of prospective taxol biomimetics and several of these active hybrid structures may provide molecular probes for exploring the molecular recognition details of the taxoid binding site on β-tubulin.

Experimental Section

Full experimental details and characterization data for all hybrids and intermediates can be found in the Supporting Information.

Double hybrid **5**: R_f 0.39 (100% EtOAc); $\mathbf{R_t}$ 28 min (10% IPA / hexane); $[\alpha]_D^{20}$ +71.6 (*c* = 0.27); **IR** (Thin film) ν_{max} = 3385, 2963, 2929, 2873, 1713, 1640, 1454, 1413, 1379; **^{1}H NMR** (700 MHz, CD_3OD) δ = 6.62 (1H, dt, *J* = 17.0, 10.6 Hz, H25), 6.08 (1H, t, *J* = 10.9 Hz, H3), 5.98 (1H, t, *J* = 10.9 Hz, H24), 5.65 (1H, d, *J* = 11.8 Hz, H2), 5.57 (1H, dd, *J* = 9.0, 10.9 Hz, H11), 5.30 (1H, t, *J* = 10.1 Hz, H10), 5.19 (1H, *br* t, *J* = 9.0 Hz, H23), 5.16 (1H, d, *J* = 17.0 Hz, H26a), 5.08 (1H, d, *J* = 10.1 Hz, H26b), 4.88 (1H, *br* d, *J* = 4.9 Hz, H21), 4.83 (1H, d, *J* = 10.2 Hz, H15), 4.50 (1H, *br* d, *J* = 8.3 Hz, H9), 4.12 (1H, *br* dd, *J* = 3.9, 9.7 Hz, H7), 3.55 (1H, *br* s, H4), 3.37 – 3.32 (1H, m, H5), 3.07 – 3.02 (2H, m, H13, H22), 2.98 (1H, *br* s, H19), 2.56 (1H, quin., *J* = 7.7 Hz, H12), 2.40 – 2.35 (1H, m, H14), 2.32 (1H, *br* s, H17a), 2.11 (1H, *br* s, H18), 1.96 – 1.91 (1H, m, H20), 1.78 (1H, sex., *J* = 7.2 Hz, H6), 1.65 (3H, s, Me16), 1.53 (1H, d, *J* = 12.6 Hz, H17b), 1.36 (1H, ddd, *J* = 2.6, 11.4, 13.8 Hz, H8a), 1.24 (1H, dd, *J* = 2.9, 10.7 Hz, H8b), 1.05 (3H, d, *J* = 7.2 Hz, Me12), 0.97 (3H, d, *J* = 6.8 Hz, Me20), 0.95 (3H, d, *J* = 6.8 Hz, Me4), 0.93 (3H, d, *J* = 6.8 Hz, Me14), 0.91 (3H, d, *J* = 6.8 Hz, Me22), 0.84 (3H, d, *J* = 7.0 Hz, Me6), 0.64 (3H, d, *J* = 6.3 Hz, Me18); **^{13}C NMR** (175 MHz, CD_3OD) δ = 173.0 (C1), 167.6 (C16), 135.3 (C10), 134.5 (C23), 133.6 (C25), 131.4 (C24), 131.3 (C15), 131.0 (C11), 119.6 (C2), 118.4 (C26), 80.8 (C13), 78.6 (C5), 78.1 (C21), 77.0 (C19), 68.2 (C7), 65.1 (C9), 43.4 (C6), 38.6 (C17), 38.4 (C8), 38.3 (2C, C14, C20), 37.2 (C4), 35.8 (C12), 35.5 (C22), 32.8 (C18), 23.2 (Me16), 19.9 (Me12), 19.3 (Me22), 17.8 (Me14), 12.8 (Me4), 12.0 (Me6), 11.7 (Me18), 10.1 (Me20); **HRMS** (ES+) Calcd. for $C_{34}H_{56}O_7Na$ $[M+Na]^+$ 599.3918. Found: 599.3923.

Double hybrid **12**: R_f 0.48 (100% EtOAc); $\mathbf{R_t}$ 15 min (10% IPA / hexane); $[\alpha]_D^{20}$ −106.9 (*c* 0.38, $CHCl_3$); **IR** (neat, cm^{-1}) υ_{max} = 3406, 2965, 2931, 1687, 1638, 1453; **^{1}H NMR** (500 MHz, C_6D_6) δ = 7.51 (1H, dd, *J* = 11.2, 15.6 Hz, H4), 6.64 (1H, ddd, *J* = 10.5, 10.6, 16.8 Hz, H25), 6.25 (1H, t, *J* = 11.6 Hz, H3), 6.02 (1H, t, *J* = 11.0 Hz, H24), 5.88 (1H, dd, *J* = 7.7, 15.5 Hz, H5), 5.63 (1H, d, *J* = 11.7 Hz, H2), 5.53 – 5.64 (2H, m, H10, H11), 5.40 (1H, t, *J* = 10.5 Hz, H23), 5.30 (1H, dd, *J* = 3.0, 8.6 Hz, H21), 5.12 (1H, d, *J* = 17.0 Hz, H26a), 5.00 (2H, t, *J* = 12.0 Hz, H15, H26b), 4.66 (1H, dq, *J* = 4.0, 7.8 Hz, H9), 4.01 (1H, d, *J* = 10.6 Hz, H7), 3.27 (1H, dd, *J* = 2.4, 8.6 Hz, H19), 3.04 – 3.13 (2H, m, H13, H22), 2.65 – 2.78 (2H, m, H12, H14), 2.30 – 2.38 (2H, m, H6, H18), 2.00 – 2.18 (3H, m, H17a, H17b, H20), 1.79 (3H, s, Me16), 1.67 (1H, ddd, *J* = 3.8, 10.4, 14.3 Hz, H8a), 1.46 (1H, ddd, *J* = 2.3, 7.8, 14.1 Hz, H8b), 1.25 (3H, d, *J* = 6.7 Hz, Me20), 1.17 (3H, d, *J* = 6.8 Hz, Me6), 1.07 (3H, d, *J* = 6.9 Hz, Me12), 1.05 (3H, d, *J* = 7.0 Hz, Me14), 0.96 (3H, d, *J* = 6.6 Hz, Me18), 0.87 (3H, d, *J* = 6.6 Hz, Me22); **^{13}C NMR** (125 MHz, C_6D_6) δ = 166.2 (C1), 144.9 (C5), 143.2 (C3), 134.8 (C23), 134.5 (C10), 134.0 (C11), 132.7 (C25), 132.6 (C16), 130.4 (C24), 128.6 (C15), 127.9 (C4), 118.1 (C2), 118.0 (C26), 79.5 (C13), 76.8 (C21), 74.8 (C19), 71.1 (C7), 66.0 (C9), 43.3 (C6), 40.8 (C8), 37.8 (C14), 37.6 (C17), 37.2 (C20), 35.4 (C22), 35.2 (C12), 31.8 (C18), 23.2 (Me16), 20.0 (Me12), 19.3 (Me14), 17.2 (Me22), 15.6 (Me6), 12.7 (Me18), 10.8 (Me20); **HRMS** (ESI+) Calcd. for $C_{33}H_{53}O_6$ $[M+H]^+$: 545.3842. Found: 545.3864.

Double hybrid **23**: R_f 0.37 (100% EtOAc); $\mathbf{R_t}$ 12 min (10% IPA / hexane); −64.6 $[\alpha]_D^{20}$ (*c* 0.3, $CHCl_3$); **IR** (neat, cm^{-1}) υ_{max} = 3395, 2963, 2928, 1683, 1638, 1454, 1407, 1378; **^{1}H NMR** (500 MHz, C_6D_6) δ = 7.43 (1H, dd, *J* = 11.2 Hz, H4), 6.56 (1H, dt, *J* = 10.9, 16.9 Hz, H25), 6.21 (1H, t, *J* = 11.5 Hz, H3), 6.10 (1H, t, *J* = 10.7 Hz, H24), 5.74 (1H, dd, *J* = 8.8, 15.4 Hz, H5), 5.67 (1H, d, *J* = 11.7 Hz, H2), 5.60 (1H, t, *J* = 10.7 Hz, H23), 5.49 (1H, t, *J* = 6.2 Hz, H21), 5.19 (1H, d, *J* = 16.8 Hz, H26b), 5.04 (1H, d, *J* = 10.4 Hz, H26a), 4.92 (1H, d, *J* = 10.6 Hz, H15), 3.65 – 3.71 (2H, m, H7, H9), 3.35 (1H, t, *J* = 5.4 Hz, H19), 3.14 (1H, *ddd*, J = 6.7, 13.4, 18.0 Hz, H22), 3.04 (1H, dd, *J* = 1.7, 7.7 Hz, H13), 2.62 (1H, ddd, *J* = 6.6, 13.7, 17.2 Hz, H14), 2.35 – 2.43 (1H, m, H6), 2.08 – 2.15 (1H, m, H20), 2.05 (2H, d, *J* = 6.8 Hz, H17a, H17b), 1.93 (12H, dt, *J* = 7.0, 13.5 Hz, H18), 1.87 (1H, *br* s, H10a), 1.71 (2H, t, *J* = 7.2 Hz, H10b, H11a), 1.65 (3H, s, Me16), 1.49 – 1.55 (2H, m, H11b, H12), 1.40 –

1.45 (1H, m, H8a), 1.17 – 1.22 (1H, m, H8b), 1.14 (3H, d, *J* = 6.8 Hz, Me20), 1.01 (3H, *obs* d, *J* = 6.3 Hz, Me14), 1.00 (3H, *obs* d, *J* = 6.9 Hz, Me6), 0.98 (3H, *obs* d, *J* = 7.1 Hz, Me22), 0.93 (3H, *obs* d, *J* = 6.8 Hz, Me12), 0.92 (3H, *obs* d, *J* = 6.4 Hz, Me18); **^{13}C NMR** (500 MHz, C_6D_6) δ = 166.5 (C1), 145.0 (C5), 142.2 (C3), 34.4 (C23), 133.4 (C16), 132.6 (C25), 130.2 (C24), 129.9 (C15), 129.3 (C4), 118.7 (C2), 118.2 (C26), 81.0 (C13), 78.1 (C21), 75.3 (C19), 72.5 (C7), 70.0 (C9), 44.0 (C6), 40.7 (C12), 37.9 (C20), 37.1 (C14), 36.3 (C8), 35.8 (C17), 34.8 (C22), 32.9 (C18), 32.0 (C10), 25.3 (C11), 23.0 (Me16), 18.8 (Me14), 17.7 (Me22), 17.2 (Me16), 14.4 (Me18), 14.0 (Me12), 10.4 (Me20); **HRMS** (ESI+) calc. for $C_{33}H_{55}O_6$ $[M+H]^+$: 547.3999. Found: 547.4013.

Acetonide **18**: R_f 0.66 (40% EtOAc); **R_t** 16 min (25% EtOAc / hexane); $[\alpha]_D^{20}$ −20.0 (*c* 0.06, $CHCl_3$); **IR** (neat, cm^{-1}) υ_{max} = 3395, 2923, 2853, 1713, 1641, 1456; **^{1}H NMR** (500 MHz, C_6D_6) δ = 7.60 (1H, dd, *J* = 11.0, 15.0 Hz, H4), 6.67 (1H, ddd, *J* = 9.5, 10.6, 16.5 Hz, H25), 6.24 (1H, t, *J* = 11.0 Hz, H3), 5.99 (1H, t, *J* = 10.9 Hz, H24), 5.77 (1H, dd, *J* = 7.0, 15.9 Hz, H5), 5.53 – 5.68 (3H, m, H2, H10, H11), 5.31 (1H, t, *J* = 10.9 Hz, H23), 5.23 (1H, dd, *J* = 2.3, 9.1 Hz, H21), 5.10 (1H, d, *J* = 16.8 Hz, H26a), 5.03 (1H, d, *J* = 10.5 Hz, H26b), 4.95 (1H, d, *J* = 10.5 Hz, H15), 4.58 (1H, dq, *J* = 6.4, 9.9 Hz, H9), 3.87 (1H, ddd, *J* = 3.2, 6.4, 9.0 Hz, H7), 3.08 (1H, d, *J* = 9.5 Hz, H19), 3.03 (1H, dq, *J* = 6.4, 14.9 Hz, H22), 2.95 (1H, dd, *J* = 3.7, 7.8 Hz, H13), 2.66 – 2.74 (1H, m, H12), 2.62 (1H, q, *J* = 8.2 Hz, H14), 2.50 – 2.56 (1H, m, H6), 2.43 – 2.50 (1H, m, H18), 2.28 (1H, t, *J* = 12.3 Hz, H17a), 1.98 (1H, ddd, *J* = 2.8, 7.3, 9.6 Hz, H20), 1.89 – 1.95 (1H, m, H17b), 1.86 (3H, s, Me16), 1.79 (1H, ddd, *J* = 5.9, 9.1, 14.9 Hz, H8a), 1.41 (3H, s, $C(CH_3)_2$), 1.38 (3H, s, $C(CH_3)_2$), 1.28 – 1.35 (1H, m, H8b), 1.24 (3H, d, *J* = 6.8 Hz, Me6), 1.15 (3H, d, *J* = 7.2 Hz, Me20), 1.06 (3H, d, *J* = 6.9 Hz, Me12), 1.03 (3H, d, *J* = 6.9 Hz, Me14), 0.95 (3H, d, *J* = 6.8 Hz, Me18), 0.80 (3H, d, *J* = 7.3 Hz, Me22); **^{13}C NMR** (125 MHz, C_6D_6) δ = 165.8, 144.3, 143.8, 135.0, 134.6, 132.9, 132.8, 131.9, 130.3, 127.8, 117.8, 117.7, 100.6, 79.9, 76.0, 75.2, 68.2, 67.9, 63.9, 40.6, 37.6, 37.5, 36.2, 35.1, 34.2, 31.3, 25.9, 25.2, 24.7, 23.3, 19.5, 19.3, 17.0, 11.6, 10.4; **HRMS** (ESI +) Calcd. for $C_{36}H_{56}O_6Na$ $[M+Na]^+$: 607.3975. Found: 607.3994.

Triple hybrid **31**: **R_f** 0.63 (80% EtOAc / P.E.); **R_t** 15.0 min (8% IPA / hexane); $[\alpha]_D^{20}$ +23.3 (*c* 0.03, $CHCl_3$); **IR** (neat, cm^{-1}) υ_{max}= 3348, 2923, 2853, 1711, 1647, 1520, 1461; **^{1}H NMR** (500 MHz, d7-DMF) δ = 8.83 (1H, d, *J* = 8.9 Hz, NH), 8.00 (2H, d, *J* = 8.3 Hz, Ar), 7.60 (2H, d, *J* = 7.8 Hz, Ar), 7.57 (2H, d, *J* = 7.6 Hz, Ar), 7.50 (2H, t, *J* = 7.7 Hz, Ar), 7.37 – 7.43 (1H, m, Ar), 7.32 (1H, t, *J* = 7.5 Hz, Ar), 7.23 (1H, t, *J* = 12.3 Hz, H4), 6.70 – 6.80 (2H, m, H3, H25), 6.24 (1H, dd, *J* = 5.8, 15.6 Hz, H5), 6.05 – 6.13 (1H, m, H24), 5.77 (1H, dd, *J* = 2.9, 9.0 Hz, H11), 5.65 – 5.72 (2H, m, H2, H3′), 5.36 (1H, d, *J* = 9.0 Hz, H23), 5.31 – 5.35 (1H, m, H7), 5.28 (2H, d, *J* = 16.3 Hz, H10, H26a), 5.18 (1H, d, *J* = 10.2 Hz, H26b), 5.07 (1H, t, *J* = 5.8 Hz, H21), 4.98 (1H, d, *J* = 10.2 Hz, H15), 4.70 (1H, d, *J* = 2.8 Hz, C13-O<u>H</u>), 4.62 (1H, d, *J* = 4.1 Hz, C19-O<u>H</u>), 4.55 – 4.61 (2H, m, H9, H2′), 3.18 – 3.26 (1H, m, H22), 3.08 – 3.16 (2H, t, *J* = 10.2 Hz, H13, H19), 2.54 – 2.61 (1H, m, H6), 2.41 – 2.49 (1H, m, H12), 2.24 – 2.32 (1H, m, H14), 2.02 – 2.08 (1H, m, H18), 1.99 (1H, q, *J* = 6.1 Hz, H20), 1.74 (3H, s, Me16), 1.55 (2H, q, *J* = 11.2 Hz, H8a, H17a), 1.37 – 1.43 (1H, m, H8b), 1.33 – 1.37 (1H, m, H17b), 1.15 (3H, d, *J* = 7.1 Hz, Me12), 1.06 (3H, d, *J* = 6.9 Hz, Me20), 1.05 (3H, d, *J* = 6.9 Hz, Me6), 0.99 (6H, t, *J* = 6.3 Hz, Me14, Me22), 0.74 (3H, d, *J* = 6.3 Hz, Me18); **HRMS** (ES^+) calc. for $C_{49}H_{66}NO_9$ $[M+H]^+$: 812.4738. Found: 812.4736.

Double hybrid **32**: **R_f** 0.56 (70% EtOAc / P.E.); **R_t** 13.5 min (7% IPA / hexane); $[\alpha]_D^{20}$ −20.0 (*c* 0.02, $CHCl_3$); **IR** (neat, cm^{-1}) ν_{max} = 3450, 2963, 2918, 1696, 1498, 1457; **^{1}H NMR** (500 MHz, C_6D_6) δ = 7.68 (1H, t, *J* = 13.5 Hz, H4), 7.38 (2H, d, *J* = 7.4 Hz, Ar), 7.11 (2H, *obs* d, *J* = 7.7 Hz, Ar), 7.05 (1H, t, *J* = 7.4 Hz, Ar), 6.66 (1H, ddd, *J* = 10.7, 10.8, 16.8 Hz, H25), 6.13 (1H, t, *J* = 11.0 Hz, H3), 5.98 (1H, t, *J* = 11.0 Hz, H24), 5.66 – 5.81 (2H, m, H7, H11), 5.63 (1H, dd, *J* = 6.1, 16.2 Hz, H5), 5.58 (1H, d, *J* = 11.3 Hz, H2), 5.45 (1H, d, *J* =

10.1 Hz, NH), 5.34 (1H, d, *J* = 10.1 Hz, H3′), 5.26 (1H, t, *J* = 10.4 Hz, H23), 5.20 (1H, dd, *J* = 2.5, 8.9 Hz, H21), 5.11 (1H, d, *J* = 16.8 Hz, H26a), 5.03 (2H, d, *J* = 10.6 Hz, H10, H26b), 4.89 (1H, d, *J* = 10.1 Hz, H15), 4.41 (1H, d, *J* = 5.5 Hz, H2′), 4.33 (1H, d, *J* = 5.1 Hz, H9), 3.11 – 3.18 (1H, m, H6), 3.05 (2H, d, *J* = 5.5 Hz, H13, C2′-OH), 2.99 (2H, t, *J* = 9.2 Hz, H19, H22), 2.71 (1H, t, *J* = 2.7 Hz, H12), 2.61 (1H, q, *J* = 6.4 Hz, H14), 2.45 – 2.56 (2H, m, H17a, H18), 1.94 (3H, s, Me16), 1.89 – 1.93 (1H, *obs* m, H20), 1.81 (1H, dt, *J* = 2.8, 13.1 Hz, H8a), 1.70 (1H, d, *J* = 11.1 Hz, H8a), 1.65 (1H, dt, *J* = 2.8, 13.0 Hz, H17b), 1.34 (3H, d, *J* = 7.1 Hz, Me12), 1.28 (9H, s, $C(CH_3)_3$), 1.10 (3H, d, *J* = 7.1 Hz, Me6), 1.08 (3H, d, *J* = 6.9 Hz, Me20), 1.06 (3H, d, *J* = 6.7 Hz, Me14), 0.88 (3H, d, *J* = 6.5 Hz, Me18), 0.77 (3H, d, *J* = 6.7 Hz, Me22); **^{13}C NMR** (125 MHz, CD_2Cl_2) δ = 173.2 (C1′), 166.3 (C1), 156.3 (^{t}BuOC(O)NHR), 143.9 (C3), 142.9 (C5), 140.4 (Ar), 134.8 (C10, C23), 133.8 (C16), 132.9 (C25), 130.5 (C24), 129.7 (C11), 129.4 (C15), 129.3 (Ar), 128.5 (Ar), 128.0 (C4), 127.4 (2C, Ar), 118.15 (C2), 118.10 (C26), 81.1 (CMe_3), 80.1 (C13), 76.7 (C21), 76.5 (C19), 75.7 (C7), 73.5 (C2′), 63.9 (C9), 56.8 (C3′), 38.7 (C6), 37.8 (C17), 37.51 (C20), 37.47 (C14), 35.3 (C12), 35.1 (C8), 35.0 (C6), 31.5 (C18), 28.6 (3C, CMe_3), 23.5 (Me16), 19.3 (Me14), 19.0 (Me12), 17.3 (Me22), 12.3 (Me6), 11.5 (Me18), 10.0 (Me20); **HRMS** (ES^+) calc. for $C_{47}H_{69}N\,O_{10}Na$ $[M+Na]^+$: 830.4819. Found: 830.4858.

Double hybrid **33**: **R_f** 0.63 (80% EtOAc / P.E.); **R_t** 9.1 min (8% IPA / hexane); $[\alpha]_D^{20}$ +6.6 (*c* 0.03, $CHCl_3$); **IR** (neat, cm^{-1}) υ_{max} = 3363, 2922, 2853, 1715, 1655, 1517, 1457; **^{1}H NMR** (500 MHz, d7-DMF) δ = 8.71 (1H, d, *J* = 9.1 Hz, NH), 7.99 (2H, d, *J* = 7.3 Hz, Ar), 7.55 – 7.61 (3H, m, Ar), 7.52 (2H, t, *J* = 7.8 Hz, Ar), 7.41 (2H, t, *J* = 7.5 Hz, Ar), 7.33 (1H, t, *J* = 7.3 Hz, Ar), 7.20 (1H, t, *J* = 13.1 Hz, H4), 6.72 – 6.81 (2H, m, H3, H25), 6.24 (1H, dd, *J* = 6.1, 15.8 Hz, H5), 6.09 (1H, t, *J* = 10.9 Hz, H24), 6.05 (1H, d, *J* = 9.5 Hz, C2′-OH), 5.79 (1H, t, *J* = 9.5 Hz, H11), 5.73 (1H, t, *J* = 9.2 Hz, H9), 5.68 – 5.71 (1H, *obs* m, H3′), 5.67 (1H, *obs* d, *J* = 10.4 Hz, H2), 5.38 (1H, t, *J* = 10.7 Hz, H23), 5.30 (1H, *obs* d, *J* = 15.8 Hz, H26a), 5.29 (1H, *obs* t, *J* = 9.6 Hz, H10), 5.20 (1H, d, *J* = 10.4 Hz, H26b), 5.07 (1H, t, *J* = 5.8 Hz, H21), 4.91 (1H, d, *J* = 10.2 Hz, H15), 4.81 (1H, d, *J* = 5.6 Hz, C13-OH), 4.71 (1H, d, *J* = 5.3 Hz, C19-OH), 4.63 (1H, t, *J* = 4.4 Hz, H2′), 4.53 (1H, d, *J* = 5.3 Hz, C7-OH), 3.21 – 3.28 (1H, m, H22), 3.13 – 3.18 (1H, m, H19), 3.10 (1H, dd, *J* = 6.1, 9.5 Hz, H13), 2.57 (1H, q, *J* = 6.1 Hz, H6), 2.50 (1H, t, *J* = 7.5 Hz, H12), 2.36 (1H, q, *J* = 8.5 Hz, H14), 2.00 (2H, q, *J* = 6.1 Hz, H18, H20), 1.69 (3H, s, Me16), 1.57 (1H, d, *J* = 12.1 Hz, H17a), 1.48 (1H, t, *J* = 11.2 Hz, H8a), 1.41 (1H, dt, *J* = 3.2, 10.4 Hz, H8b), 1.25 – 1.31 (1H, m, H17b), 1.13 (3H, d, *J* = 7.1 Hz, Me12), 1.05 (6H, t, *J* = 6.3 Hz, Me6, Me20), 0.99 (3H, d, *J* = 6.8 Hz, Me22), 0.96 (3H, d, *J* = 6.6 Hz, Me14), 0.74 (3H, d, *J* = 6.7 Hz, Me18); **^{13}C NMR** (125 MHz, d7-DMF) δ = 172.0, 167.8, 166.8, 145.9, 144.0, 140.9, 135.1, 134.1, 133.7, 133.5, 133.1, 132.3, 130.7, 130.6, 129.5, 129.1 (2C), 129.0 (2C), 128.2 (2C), 128.1 (2C), 128.0, 127.3, 118.2, 117.8, 79.1, 78.8, 75.4, 75.0, 70.2, 68.1, 56.9, 43.0, 38.0, 37.8, 37.3, 36.6, 34.6, 32.7, 23.2 (2C), 23.1, 19.4, 18.7, 18.0, 14.3, 13.6, 12.3, 10.0; **HRMS** (ES^+) calc. for $C_{49}H_{66}NO_9$ $[M+H]^+$: 812.4738. Found: 812.4734.

Double hybrid **34**: **R_f** 0.56 (70% EtOAc / P.E.); **R_t** 9.5 min (7% IPA / hexane); $[\alpha]_D^{20}$ +6.0 (*c* 0.03, $CHCl_3$); **IR** (neat, cm^{-1}) υ_{max} = 3433, 2963, 2920, 1694, 1498, 1456; **^{1}H NMR** (500 MHz, CD_2Cl_2) δ = 7.36 – 7.42 (4H, m, Ar), 7.29 – 7.34 (1H, m, Ar), 7.28 (1H, dd, *J* = 4.4, 15.4 Hz, H4), 6.64 (1H, ddd, *J* = 10.9, 11.0, 16.9 Hz, H25), 6.54 (1H, t, *J* = 11.0 Hz, H3), 6.08 (1H, dd, *J* = 7.0, 15.6 Hz, H5), 5.99 (1H, t, *J* = 11.0 Hz, H24), 5.65 (1H, *obs* dd, *J* = 8.6, 11.0 Hz, H11), 5.58 – 5.63 (1H, m, H9), 5.50 (2H, d, *J* = 11.2 Hz, H2, NH), 5.27 – 5.35 (2H, m, H10, H23), 5.15 – 5.20 (2H, m, H26a, H3′), 5.09 (1H, d, *J* = 10.0 Hz, H26b), 4.99 (2H, dd, *J* = 2.7, 9.0 Hz, H15, H21), 4.44 (1H, d, *J* = 4.5 Hz, H2′), 4.00 (1H, d, *J* = 9.8 Hz, H7), 3.68 (1H, *br* s, OH), 3.24 (1H, dd, *J* = 3.4, 8.5 Hz, H13), 3.13 (1H, d, *J* = 4.6 Hz, C2′-OH), 3.06 (2H, d, *J* = 7.6 Hz, H19, H22), 2.62 – 2.68 (1H, m, H12), 2.49 – 2.58 (2H, m, H6, H14), 2.05 – 2.13 (2H, m, H17a, H18), 1.95 (1H, ddd, *J* = 2.5, 3.0, 6.7 Hz, H20), 1.75 (1H,

d, *J* = 7.8 Hz, H17b), 1.65 (3H, s, Me16), 1.47 – 1.60 (2H, m, H8a, H8b), 1.42 (9H, s, $C(CH_3)_3$), 1.16 (6H, t, *J* = 6.9 Hz, Me6, Me12), 1.12 (3H, d, *J* = 6.7 Hz, Me20), 1.01 (3H, d, *J* = 6.7 Hz, Me22), 0.99 (3H, d, *J* = 6.8 Hz, Me14), 0.74 (3H, d, Me18); **^{13}C NMR** (125 MHz, CD_2Cl_2) δ = 173.0 (C1′), 166.4 (C1), 156.3 (^{t}BuOC(O)NHR), 145.7 (C5), 143.8 (C3), 139.9 (Ar), 135.1 (C23), 134.4 (C16), 133.2 (C11), 132.9 (C25), 130.3 (C24), 129.5 (C10), 129.2 (2C, Ar), 129.0 (C15), 128.3 (Ar), 127.9 (C4), 127.3 (2C, Ar), 118.0 (C26), 117.7 (C2), 81.1 (CMe3), 79.9 (C13), 76.7 (C21), 75.7 (C19), 73.6 (C2′), 72.3 (C9), 69.2 (C7), 56.6 (C3′), 43.7 (C6), 37.7 (C20), 37.4 (3C, C8, C14, C17), 35.5 (C12), 35.1 (C22), 31.6 (C18), 28.6 (CMe_3), 23.3 (Me16), 19.2 (Me14), 17.7 (Me12), 17.4 (Me22), 13.8 (Me6), 12.0 (Me18), 10.5 (Me20); **HRMS** (ES^+) calc. for $C_{47}H_{70}NO_{10}$ $[M+H]^+$: 808.5000. Found: 808.5028.

Double hybrid **38**: **R_f** 0.54 (70% EtOAc / P.E.); **R_t** 20.0 min (4.5% IPA / hexane); $[\alpha]_D^{20}$ −109.4 (*c* 0.17, $CHCl_3$); **IR** (neat, cm^{-1}) υ_{max} = 3456, 2961, 2928, 1699, 1638, 1457; **^{1}H NMR** (500 MHz, CD_2Cl_2) δ = 7.14 (1H, dd, *J* = 11.3, 15.8 Hz, H4), 6.60 (1H, dddd, *J* = 0.9, 10.6, 11.0, 16.9 Hz, H25), 6.49 (1H, dt, *J* = 0.6, 11.4 Hz, H3), 5.98 (1H, *obs* dd, *J* = 6.4, 8.9 Hz, H5), 5.94 (1H, *obs* t, *J* = 4.1 Hz, H24), 5.57 (1H, t, *J* = 10.0 Hz, H11), 5.45 (1H, *obs* d, *J* = 11.6 Hz, H2), 5.45 (1H, *obs* dd, *J* = 9.4, 11.2 Hz, H10), 5.29 (1H, t, *J* = 10.4 Hz, H23), 5.15 (1H, dt, *J* = 2.0, 16.7 Hz, H26a), 5.06 (2H, t, *J* = 12.4 Hz, H15, H26b), 5.00 (1H, dd, *J* = 3.0, 8.8 Hz, H21), 4.22 (1H, qu, *J* = 4.5 Hz, H9), 3.84 (1H, ddd, *J* = 2.3, 4.5, 10.3 Hz, H7), 3.31 (1H, t, *J* = 6.3 Hz, H13), 3.24 (3H, s, OMe), 3.10 (1H, dd, *J* = 2.8, 8.9 Hz, H19), 3.05 (1H, q, *J* = 7.4 Hz, H22), 2.75 – 2.83 (2H, m, H12, H14), 2.49 – 2.63 (1H, *br* s, OH), 2.22 – 2.28 (1H, m, H6), 2.11 (1H, dd, *J* = 8.8, 13.5 Hz, H17a), 1.89 – 1.99 (2H, m, H18, H20), 1.83 (1H, dd, *J* = 7.2, 13.2 Hz, H17b), 1.52 – 1.57 (2H, m, H8a, H8b), 1.51 (3H, s, Me16), 1.14 (3H, d, *J* = 6.8 Hz, Me20), 1.11 (3H, d, *J* = 6.8 Hz, Me6), 1.08 (3H, d, *J* = 6.8 Hz, Me12), 1.01 (3H, d, *J* = 6.7 Hz, Me 22), 0.97 (3H, d, *J* = 6.9 Hz, Me14), 0.81 (3H, d, *J* = 6.5 Hz, Me18); **^{13}C NMR** (125 MHz, CD_2Cl_2) δ = 166.7 (C1), 145.4 (C5), 142.6 (C3), 135.25 (C16), 135.19 (2C, C11, C23), 132.8 (C25), 132.1 (C10), 130.2 (C24), 128.9 (C4), 127.9 (C15), 118.4 (C2), 118.0 (C26), 79.4 (C13), 77.2 (C21), 75.6 (C9), 73.7 (C19), 71.9 (C7), 56.6 (OMe), 45.0 (C6), 40.6 (C8), 37.82 (C20), 37.76 (C14), 36.9 (C17), 35.5 (C22), 35.2 (C12), 31.7 (C18), 23.1 (Me16), 19.5 (Me12), 19.1 (Me14), 17.5 (Me22), 16.3 (Me6), 13.1 (Me8), 11.2 (Me20); **HRMS** (ES^+) calc. for $C_{34}H_{55}O_6$ $[M+H]^+$: 559.3999. Found: 599.3998.

Double hybrid **44**: **R_f** 0.37 (70% EtOAc / P.E.); **R_t** 34.9 mins (6% IPA / hexane); $[\alpha]_D^{20}$ −24.4 (*c* 0.09, $CHCl_3$); **IR** (neat, cm^{-1}) υ_{max} = 3402, 2928, 1672, 1638, 1451; **^{1}H NMR** (500 MHz, CD_2Cl_2) δ = 7.26 (1H, dd, *J* = 11.3, 15.8 Hz, H4), 6.64 (1H, dddd, *J* = 0.9, 10.7, 10.8, 16.9 Hz, H25), 6.52 (1H, t, *J* = 11.4 Hz, H3), 6.02 (1H, dd, *J* = 6.6, 9.2 Hz, H5), 5.99 (1H, t, *J* = 10.6 Hz, H24), 5.58 (1H, dd, *J* = 9.0, 11.4 Hz, H11), 5.49 (1H, d, *J* = 11.4 Hz, H2), 5.37 (1H, dd, *J* = 8.4, 11.3 Hz, H10), 5.29 (1H, *obs* t, *J* = 10.6 Hz, H23), 5.18 (1H, dd, *J* = 1.9, 16.8 Hz, H26a), 5.10 (1H, d, *J* = 10.2 Hz, H26b), 4.98 (1H, dd, *J* = 3.5, 8.4 Hz, H21), 4.95 (1H, d, *J* = 9.9 Hz, H15), 4.45 (1H, t, *J* = 8.0 Hz, H9), 3.52 (1H, ddd, *J* = 3.5, 6.4, 6.9 Hz, H7), 3.39 (3H, s, OMe), 3.21 (1H, dd, *J* = 3.3, 8.4 Hz, H13), 3.02 – 3.09 (2H, m, H19, H22), 2.77 (1H, q, *J* = 6.4 Hz, H6), 2.63 (1H, tt, *J* = 1.7, 8.0 Hz, H12), 2.48 (1H, q, *J* = 9.5, H14), 1.99 – 2.09 (2H, m, H17a, H18), 1.94 (1H, ddd, *J* = 1.6, 3.6, 6.8 Hz, H20), 1.67 – 1.72 (1H, m, H17b), 1.64 (3H, s, Me16), 1.37 – 1.43 (1H, m, H8a), 1.31 – 1.36 (1H, m, H8b), 1.08 (9H, d, *J* = 7.3 Hz, Me6, Me12, Me20), 0.99 (6H, t, *J* = 6.8 Hz, Me14, Me22), 0.72 (3H, d, *J* = 6.1 Hz, Me18); **^{13}C NMR** (125 MHz, CD_2Cl_2) δ = 166.5 (C1), 145.6 (C5), 144.0 (C3), 134.8 (C23), 134.5 (C16), 134.3 (C10), 132.9 (C25), 131.8 (C11), 130.4 (C24), 128.9 (C15), 127.9 (C4), 118.1 (C26), 117.4 (C2), 80.3 (C7), 80.1 (C13), 76.9 (C21), 75.7 (C19), 65.6 (C9), 58.3 (OMe), 39.1 (C6), 38.2 (C8), 37.59 (C14), 37.55 (C20), 37.3 (C17), 35.4 (C12), 35.1 (C19), 31.7 (C18), 23.2 (Me16), 19.6 (Me22), 19.3 (Me14), 17.5 (Me20),

13.5 (Me6), 12.2 (Me18), 10.3 (Me20); **HRMS** (ES^+) calc. for $C_{34}H_{55}O_6$ $[M+H]^+$: 559.3999. Found: 559.4005.

Double hybrid **36**: R_f 0.50 (50% EtOAc); R_t 32 mins (2.5% IPA / hexane); $[\alpha]_D^{20}$ −5.0 (*c* 0.10, $CHCl_3$); **IR** (neat, cm^{-1}) υ_{max} = 3435, 2962, 2930, 1713, 1639, 1599; **^{1}H NMR** (500 MHz, CD_2Cl_2) δ = 7.23 (1H, dd, *J* = 10.9, 15.2 Hz, H4), 6.64 (1H, dddd, *J* = 1.0, 10.7, 10.8, 16.8 Hz, H25), 6.52 (1H, t, *J* = 11.3 Hz, H3), 6.02 (1H, dd, *J* = 6.6, 9.1 Hz, H5), 5.99 (1H, t, *J* = 10.7 Hz, H24), 5.69 (1H, t, *J* = 8.4, 11.2 Hz, H11), 5.48 (1H, d, *J* = 11.3 Hz, H2), 5.29 (1H, t, *J* = 10.3 Hz, H23), 5.16 – 5.21 (1H, m, H10), 5.10 (1H, d, *J* = 10.3 Hz, H26a), 4.98 (1H, dd, *J* = 3.5, 8.4 Hz, H21), 4.94 (1H, d, *J* = 10.1 Hz, H15), 3.96 (1H, dt, *J* = 3.9, 9.6 Hz, H9), 3.50 (1H, dt, *J* = 3.4, 10.4 Hz, H7), 3.36 (3H, s, OMe), 3.21 (3H, s, OMe), 3.20 – 3.24 (1H, *obs* m, H13), 3.02 – 3.08 (2H, m, H19, H22), 2.78 (1H, q, *J* = 6.2 Hz, H6), 2.46 – 2.55 (2H, m, H12, H14), 2.11 (2H, d, *J* = 7.8 Hz, H17a, H17b), 1.94 (1H, ddd, *J* = 1.7, 3.8, 7.0 Hz, H20), 1.59 – 1.67 (1H, *obs* m, H18), 1.64 (3H, s, Me16), 1.19 – 1.29 (2H, m, H8a, H8b), 1.11 (3H, d, *J* = 7.1, Me12) 1.09 (3H, d, *J* = 6.9 Hz, Me20) 1.05 (3H, d, *J* = 6.9 Hz, Me6), 0.99 (3H, d, *J* = 6.6 Hz, Me22), 0.98 (3H, d, *J* = 6.6 Hz, Me14), 0.71 (3H, d, *J* = 6.2 Hz, Me18); **^{13}C NMR** (125 MHz, CD_2Cl_2) δ = 166.4 (C1), 145.7 (C5), 143.9 (C3), 134.8 (C23), 134.1 (C16), 133.5 (C10), 132.9 (C25), 132.5 (C11), 130.4 (C24), 129.0 (C15), 127.6 (C4), 118.0 (C26), 117.4 (C2), 80.2 (C13), 79.4 (C7), 76.4 (C21), 75.9 (C19), 74.1 (C9), 58.1 (OMe), 56.4 (OMe), 38.9 (C6), 37.53 (C18, C20), 37.48 (C17), 37.3 (C14), 36.2 (C8), 35.1 (C22), 34.9 (C12), 23.3 (Me16), 19.3 (Me14), 18.9 (Me12), 17.4 (Me22), 12.6 (Me6), 12.0 (Me18), 10.3 (Me20); **HRMS** (ESI+) Calcd. for $C_{35}H_{56}O_6Na$ $[M+Na]^+$: 595.3975. Found: 595.3990.

Triple hybrid **39**: R_f 0.41 (60% EtOAc / P.E.); R_t 15.5 min (6% IPA / hexane); $[\alpha]_D^{20}$ −56.9 (*c* 0.13, $CHCl_3$); **IR** (neat, cm^{-1}) υ_{max} = 3415, 2962, 2926, 1713, 1654, 1603, 1518, 1485, 1454; **^{1}H NMR** (500 MHz, CD_2Cl_2) δ = 7.79 (2H, d, *J* = 7.7 Hz, Ar), 7.54 (1H, t, *J* = 7.6 Hz, Ar), 7.43 – 7.49 (4H, m, Ar), 7.40 (2H, t, *J* = 7.6 Hz, Ar), 7.34 (1H, d, *J* = 7.6 Hz, Ar), 7.30 (1H, d, *J* = 8.8 Hz, NH), 7.19 (1H, dd, *J* = 11.3, 15.6 Hz, H4), 6.61 (1H, ddd, *J* = 10.5, 10.8, 16.7 Hz, H25), 6.50 (1H, t, *J* = 11.6 Hz, H3), 5.97 (1H, t, *J* = 11.0 Hz, H24), 5.87 (1H, dd, *J* = 8.2, 15.8 Hz, H5), 5.70 (1H, dd, *J* = 1.5, 8.8 Hz, H3′), 5.52 (1H, *obs* t, *J* = 9.3 Hz, H11), 5.51 (1H, *obs* d, *J* = 11.8 Hz, H2), 5.34 – 5.38 (1H, m, H7), 5.28 (1H, t, *J* = 10.1 Hz, H23), 5.18 (1H, d, *J* = 7.4 Hz, H15), 5.15 (1H, *obs* t, *J* = 9.6 Hz, H10), 5.13 (1H, d, *J* = 14.5 Hz, H26a), 5.06 (1H, d, *J* = 10.2 Hz, H26b), 4.97 (1H, dd, *J* = 2.6, 9.1 Hz, H21), 4.64 (1H, s, H2′), 3.79 (1H, dd, *J* = 7.8, 14.7 Hz, H9), 3.47 (1H, d, *J* = 2.0 Hz, C2′-O<u>H</u>), 3.21 (1H, t, *J* = 4.8 Hz, H13), 3.02 – 3.08 (2H, m, H19, H22), 2.95 (3H, s, OMe), 2.63 (1H, dt, *J* = 2.8, 7.1 Hz, H6), 2.48 – 2.58 (2H, m, H12, H14), 1.98 – 2.05 (2H, m, H17a, H18), 1.95 (1H, ddd, *J* = 2.5, 6.8, 9.0 Hz, H20), 1.86 – 1.91 (1H, m, H17b), 1.60 (2H, t, *J* = 7.1 Hz, H8a, H8b), 1.57 (3H, d, *J* = 1.0 Hz, Me16), 1.14 (3H, d, *J* = 6.8 Hz, Me20), 1.00 (6H, d, *J* = 6.8 Hz, Me6, Me22), 0.95 (6H, t, *J* = 7.2 Hz, Me12, Me14), 0.78 (3H, d, *J* = 6.5 Hz, Me18); **^{13}C NMR** (125 MHz, CD_2Cl_2) δ = 172.3 (Ph<u>C</u>(O)NHR), 167.3 (C1′), 166.5 (C1), 142.9 (C3), 142.7 (C5), 139.9 (Ar), 136.3 (C11), 135.0 (C23), 134.0 (Ar), 132.8 (C25), 132.7 (C16), 132.6 (Ar), 131.8 (C10), 130.7 (C15), 130.3 (C24), 129.4 (C4), 129.2 (3C, Ar), 128.5 (Ar), 127.7 (2C, Ar), 127.3 (2C, Ar), 118.8 (C2), 118.0 (C26), 79.3 (C13), 76.9 (C21), 76.1 (C7), 74.3 (C2′), 74.2 (C19), 73.0 (C9), 56.2 (OMe), 55.3 (C3′), 41.5 (C6), 37.6 (C20), 37.3 (C8), 37.2 (C12), 37.1 (C17), 35.5 (C14), 35.4 (C22), 31.5 (C18), 23.1 (Me16), 18.2 (Me14), 17.4 (Me12), 17.3 (Me22), 15.2 (Me6), 12.7 (Me18) 11.1 (Me20); **HRMS** (ES^+) calc. for $C_{50}H_{68}NO_9$ $[M+H]^+$: 826.4894. Found: 826.4908.

Triple hybrid **40**: R_f 0.54 (60% EtOAc / P.E.); R_t 15.5 mins (6% IPA / hexane); $[\alpha]_D^{20}$ −22.1 (*c* 0.14, $CHCl_3$); **IR** (neat, cm^{-1}) υ_{max} = 3432, 2925, 2853, 1716, 1497, 1457; **^{1}H NMR** (500 MHz, CD_2Cl_2) δ = 7.38 (4H, d, *J* = 4.4 Hz, Ar), 7.32 (1H, m, Ar), 7.27 (1H, dd, *J* =

11.1, 15.4 Hz, H4), 6.62 (1H, ddd, *J* = 10.4, 10.7, 16.8 Hz, H25), 6.52 (1H, t, *J* = 11.4 Hz, H3), 5.98 (1H, t, *J* = 10.9 Hz, H24), 5.92 (1H, dd, *J* = 7.3, 15.4 Hz, H5), 5.68 (1H, d, *J* = 10.2 Hz, NH), 5.65 (1H, t, *J* = 9.3 Hz, H11), 5.53 (1H, d, *J* = 11.6 Hz, H2), 5.28 (1H, t, *J* = 10.6 Hz, H23), 5.23 – 5.26 (1H, *obs* m, H7), 5.22 (1H, d, *J* = 9.4 Hz, H10), 5.17 (1H, dd, *J* = 2.0, 16.9 Hz, H26a), 5.11 (1H, d, *J* = 10.1 Hz, H15), 5.08 – 5.12 (1H, *obs* m, H3′), 5.07 (1H, d, *J* = 10.3 Hz, H26b), 4.97 (1H, dd, *J* = 3.0, 9.1 Hz, H21), 4.46 (1H, s, H2′), 3.93 (1H, dt, *J* = 5.3, 9.2 Hz, H9), 3.31 (1H, dd, *J* = 4.5, 6.1 Hz, H13), 3.23 (1H, s, C2′-O<u>H</u>), 3.17 (3H, s, OMe), 3.09 (1H, d, *J* = 9.0 Hz, H19), 3.05 (1H, dq, *J* = 7.3, 9.0 Hz, H22), 2.70 – 2.75 (1H, m, H6), 2.58 – 2.70 (2H, m, H12, H14), 2.13 – 2.22 (1H, *br* s, OH), 2.08 (1H, d, *J* = 6.9 Hz, H18), 1.88 – 2.02 (3H, m, H17a, H17b, H20), 1.63 – 1.71 (2H, m, H8a, H8b), 1.61 (3H, s, Me16), 1.38 (9H, s, $C(CH_3)_3$), 1.12 (3H, d, *J* = 6.7 Hz, Me20), 1.10 (3H, d, *J* = 6.9 Hz, Me12), 1.04 (3H, d, *J* = 7.0 Hz, Me6), 1.00 (3H, d, *J* = 6.8 Hz, Me22), 0.98 (3H, d, *J* = 6.8 Hz, Me14), 0.77 (3H, d, *J* = 6.7 Hz, Me18); **^{13}C NMR** (125 MHz, CD_2Cl_2) δ = 172.3 (C1′), 166.5 (C1), 155.8 (^{t}BuO<u>C</u>(O)NHR), 143.1 (C3), 142.9 (C5), 140.7 (Ar), 135.8 (C11), 135.0 (C23), 133.6 (C16), 132.9 (C25), 131.9 (C10), 130.3 (C24), 129.7 (C15), 129.1 (Ar), 129.0 (Ar), 128.2 (C4), 127.1 (Ar), 118.7 (C2), 118.0 (C26), 80.4 (<u>C</u>Me3), 79.8 (C13), 77.0 (C21), 75.8 (C19), 74.8 (C7), 74.7 (C2′), 74.0 (C9), 56.8 (C3′), 56.5 (OMe), 40.9 (C6), 37.6 (C20), 37.3 (C14), 36.5 (C8), 36.3 (C12), 36.2 (C17), 35.3 (C22), 31.5 (C18), 28.6 (3C, C<u>Me</u>$_3$), 23.3 (Me16), 18.8 (Me14), 18.2 (Me12), 17.4 (Me22), 14.5 (Me6), 12.4 (Me18), 10.7 (Me20); **HRMS** (ES^+) calc. for $C_{48}H_{72}NO_{10}$ $[M+H]^+$: 822.5156. Found: 822.5158.

Triple hybrid **45**: $\mathbf{R_f}$ 0.45 (60% EtOAc / P.E.); $\mathbf{R_t}$ 102 min (2% IPA / hexane); $[\alpha]_D^{20}$ +46.0 (*c* 0.05, $CHCl_3$); **IR** (neat, cm^{-1}) υ_{max} = 3427, 2959, 2934, 1711, 1651, 1518, 1486; **^{1}H NMR** (500 MHz, CD_2Cl_2) δ = 7.81 (2H, d, *J* = 7.4 Hz, Ar), 7.54 (1H, t, *J* = 7.5 Hz, Ar), 7.46 (4H, t, *J* = 6.7 Hz, Ar), 7.38 (2H, t, *J* = 7.2 Hz, Ar), 7.32 (1H, d, *J* = 7.7 Hz, Ar), 7.25 (1H, dd, *J* = 11.6, 15.4 Hz, H4), 7.19 (1H, d, *J* = 8.9 Hz, NH), 6.65 (1H, ddd, *J* = 10.3, 10.7, 16.6 Hz, H25), 6.56 (1H, t, *J* = 11.3 Hz, H3), 6.08 (1H, dd, *J* = 6.2, 15.7 Hz, H5), 6.00 (1H, t, *J* = 11.0 Hz, H24), 5.79 (1H, dt, *J* = 3.9, 10.4 Hz, H9), 5.70 (1H, d, *J* = 8.6 Hz, H3′), 5.67 (1H, *obs* dd, *J* = 8.9, 11.0 Hz, H11), 5.52 (1H, d, *J* = 11.0 Hz, H2), 5.27 – 5.31 (2H, m, H10, H23), 5.19 (1H, d, *J* = 16.9 Hz, H26a), 5.11 (1H, d, *J* = 10.7 Hz, H26b), 4.98 (1H, dd, *J* = 3.6, 8.2 Hz, H21), 4.96 (1H, d, *J* = 10.5 Hz, H15), 4.55 (1H, s, H2′), 3.36 (1H, d, *J* = 2.4 Hz, C2′-O<u>H</u>), 3.21 (1H, dd, *J* = 3.0, 8.8 Hz, H13), 3.16 (1H, ddd, *J* = 1.8, 4.2, 10.7 Hz, H7), 3.04 – 3.09 (2H, m, H19, H22), 2.98 (3H, s, OMe), 2.71 (1H, q, *J* = 6.2 Hz, H6), 2.56 (1H, t, *J* = 8.2 Hz, H12), 2.47 (1H, q, *J* = 8.8 Hz, H14), 2.13 (2H, d, *J* = 7.8 Hz, H17a, H18), 1.94 (1H, dt, *J* = 3.8, 7.8 Hz, H20), 1.66 (3H, s, Me16), 1.56 – 1.63 (2H, m, H8a, H17b), 1.37 (1H, ddd, *J* = 3.6, 11.1, 14.5 Hz, H8b), 1.10 (3H, d, *J* = 7.2 Hz, Me12), 1.09 (3H, d, *J* = 7.0 Hz, Me20), 1.00 (3H, d, *J* = 6.8 Hz, Me22), 0.97 (3H, d, *J* = 6.6 Hz, Me14), 0.94 (3H, d, *J* = 6.8 Hz, Me6), 0.70 (3H, d, *J* = 5.6 Hz, Me18); **^{13}C NMR** (125 MHz, CD_2Cl_2) δ = 172.3 (C1′), 166.7 (Ph<u>C</u>(O)NHR), 166.4 (C1), 145.4 (C5), 143.9 (C3), 140.1 (Ar), 134.7 (C23), 134.5 (Ar), 134.2 (C16), 133.7 (C11), 132.9 (C25), 132.5 (Ar), 130.4 (C24), 129.4 (C10), 129.23 (2C, Ar), 129.17 (2C, Ar), 129.1 (C15), 128.3 (Ar), 127.8 (C4), 127.6 (2C, Ar), 127.3 (2C, Ar), 118.1 (C26), 117.4 (C2), 79.8 (C13), 78.4 (C7), 76.9 (C21), 76.2 (C19), 74.5 (C2′), 71.9 (C9), 57.4 (OMe), 55.0 (C3′), 38.0 (C6), 37.6 (2C, C17, C20), 37.5 (C14), 35.5 (C12), 35.4 (C8), 35.0 (C22), 31.7 (C18), 23.3 (Me16), 19.3 (Me22), 18.2 (Me12), 17.5 (Me14), 11.90 (Me18), 11.85 (Me6), 10.2 (Me20); **HRMS** (ES^+) calc. for $C_{50}H_{68}NO_9$ $[M+H]^+$: 826.4894. Found: 826.4907.

Triple hybrid **46**: $\mathbf{R_f}$ 0.51 (60% EtOAc / P.E.); $\mathbf{R_t}$ 44 min (2% IPA / hexane); $[\alpha]_D^{20}$ +40.9 (*c* 0.11, $CHCl_3$); **IR** (neat, cm^{-1}) υ_{max} = 3421, 2964, 2925, 1710, 1639, 1496, 1454; **^{1}H NMR** (500 MHz, CD_2Cl_2) δ = 7.34 – 7.40 (4H, m, Ar), 7.27 – 7.33 (2H, m, Ar), 6.66 (1H, ddd, *J* = 10.4, 10.8, 16.6 Hz, H25), 6.60 (1H, t, *J* = 11.2 Hz, H3), 6.11 (1H, dd, *J* = 6.2, 15.9 Hz, H5), 6.01 (1H, t, *J* = 10.9 Hz, H24), 5.81 (1H, ddd, *J* = 3.2, 8.6, 11.9 Hz, H9), 5.68 (1H, dd, *J* =

8.9, 11.2 Hz, H11), 5.52 – 5.58 (2H, m, H2, NH), 5.26 – 5.31 (2H, m, H10, H23), 5.20 (1H, d, *J* = 16.7 Hz, H26a), 5.12 (2H, d, *J* = 10.2, H26B, H3′), 5.00 (1H, dd, *J* = 3.5, 8.3 Hz, H21), 4.97 (1H, d, *J* = 10.4 Hz, H15), 4.36 (1H, s, H2′), 3.30 (3H, s, OMe), 3.26 – 3.28 (1H, m, H7), 3.23 (1H, dd, *J* = 2.7, 9.0 Hz, H13), 3.15 (1H, d, *J* = 3.1 Hz, C2′-OH), 3.05 – 3.09 (2H, m, H19, H22), 2.86 (1H, q, *J* = 6.3 Hz, H6), 2.57 (1H, t, *J* = 7.7 Hz, H12), 2.47 (1H, q, *J* = 8.1 Hz, H14), 2.13 – 2.20 (2H, m, H17a, H18), 1.95 (1H, dt, *J* = 3.8, 7.8 Hz, H20), 1.74 (3H, s, Me16), 1.66 – 1.68 (1H, m, H17b), 1.63 (1H, d, *J* = 12.7 Hz, H8a), 1.39 (9H, s, $C(CH_3)_3$), 1.34 – 1.38 (1H, *obs* m, H8b), 1.13 (3H, d, *J* = 6.9 Hz, Me12), 1.10 (3H, d, *J* = 6.9 Hz, Me20), 1.05 (3H, d, *J* = 6.9 Hz, Me6), 1.00 (6H, t, *J* = 7.1 Hz, Me14, Me22), 0.71 (3H, d, *J* = 6.1 Hz, Me18); **^{13}C NMR** (125 MHz, CD_2Cl_2) δ = 172.2 (C1′), 166.4 (C1), 155.7 (^{t}BuOC(O)NHR), 145.1 (C5), 143.9 (C3), 140.8 (Ar), 134.7 (C23), 134.1 (C16), 133.3 (C11), 132.9 (C25), 130.5 (C24), 129.4 (C10), 129.2 (Ar), 129.1 (C15), 128.1 (C4), 127.7 (Ar), 126.9 (Ar), 118.2 (C26), 117.5 (C2), 80.3 (CMe_3), 79.9 (C13), 78.4 (C7), 76.9 (C21), 76.4 (C19), 74.6 (C2′), 71.6 (C9), 57.5 (OMe), 56.4 (C3′), 37.8 (C6), 37.7 (C17), 37.6 (C20), 37.5 (C14), 35.4 (C12), 35.0 (2C, C8, C22), 31.7 (C18), 28.6 (3C, CMe_3), 23.4 (Me16), 19.3 (Me14), 18.2 (Me12), 17.5 (Me22), 11.8 (Me18), 11.6 (Me6), 10.1 (Me20); **HRMS** (ES^+) calc. for $C_{48}H_{72}NO_{10}$ $[M+H]^+$: 822.5156. Found: 822.5185.

Supplementary Material

Refer to Web version on PubMed Central for supplementary material.

Acknowledgments

Financial support was provided by the EPSRC and NIH Grant no. R56 CA093455. We thank Dr J. Fernando Díaz (CSIC, Madrid) for providing AutoDock 3D structures and the figure of the lowest energy conformation of discodermolide in D2O, Dr Stuart Mickel (Novartis) for the gift of chemicals, Takeshi Fujita (Nakamura Group, University of Tokyo) for preparation of β-lactams **29** and **30**, Dr Rob Paton (Cambridge) for modelling advice, and Tara Pitts and Pat Linley (HBOI) for biological assays.

References

1. (a) Koehn FE, Carter GT. Nat. Rev. Drug Discovery 2005;4:206. (b) Butler MS. Nat. Prod. Rep 2008;25:475. [PubMed: 18497896] (c) Newman DJ, Cragg GM. J. Nat. Prod 2007;70:461. [PubMed: 17309302] (d) Paterson I, Anderson EA. Science 2005;310:451. [PubMed: 16239465] (e) Cragg, GML.; Kingston, DGI.; Newman, DJ. Anticancer Agents From Natural Products. Boca Raton: Taylor & Francis Group; 2005.
2. (a) Hamel E. Med. Chem. Rev 1996;16:207. (b) Altmann KH, Gertsch J. Nat. Prod. Rep 2007;24:327. [PubMed: 17390000]
3. Nicolaou KC, Dai WM, Guy RK. Angew. Chem 1994;1994;106:38.Angew. Chem. Int. Ed 1994;33:15.
4. Schiff PB, Fant J, Horwitz SB. Nature 1979;277:665. [PubMed: 423966]
5. Gueritte-Voegelein F, Guenard D, Lavelle F, Le Goff MT, Mangatal L, Potier P. J. Med. Chem 1991;34:992. [PubMed: 1672159]
6. Orr GA, Verdier-Pinard P, McDaid H, Horwitz SB. Oncogene 2003;22:7280. [PubMed: 14576838]
7. Hunt JT. Mol. Cancer Ther 2009;8:275. [PubMed: 19174552]
8. (a) Gunasekera SP, Gunasekera M, Longley RE, Schulte GK. J. Org. Chem 1990;55:4912. (b) Ter Haar E, Kowalski RJ, Hamel E, Lin CM, Longley RE, Gunasekera SP, Rosenkranz HS, Day BW. Biochemistry 1996;35:243. [PubMed: 8555181] (c) Kowalski RJ, Giannakakou P, Gunasekera SP, Longley RE, Day BW, Hamel E. Mol. Pharmacol 1997;52:613. [PubMed: 9380024]
9. (a) Petit GR, Cichacz ZA, Goa F, Boyd MR, Schmidt JM. J. Chem. Soc., Chem. Commun 1994:1111. (b) Isbrucker RA, Cummins J, Pomponi SA, Longley RE, Wright AE. Biochem. Pharmacol 2003;66:75. [PubMed: 12818367] (c) Paterson I, Britton R, Delgado O, Wright AE. Chem. Commun 2004:632.

10. Buey RM, Calvo E, Barasoain I, Pineda O, Edler MC, Matesanz R, Cerezo G, Vanderwal CD, Day BW, Sorensen EJ, Lopez JA, Andreu JM, Hamel E, Díaz JF. Nat. Chem. Bio 2007;3:117. [PubMed: 17206139]
11. Buey RM, Barasoain I, Jackson E, Meyer A, Giannakakou P, Paterson I, Mooberry S, Andreu JM, Díaz JF. Chem. Biol 2005:1269. [PubMed: 16356844]
12. (a) Honore S, Kamath K, Braguer D, Horwitz SB, Wilson L, Briand C, Jordan MA. Cancer Res 2004;64:4957. [PubMed: 15256469] (b) Huang GS, Barcons LL, Freeze BS, Smith AB III, Goldberg GL, Horwitz SB, McDaid HM. Clin. Cancer Res 2006;12:298. [PubMed: 16397055]
13. For reviews on discodermolide and its analogues, see: (a) Florence GJ, Gardner NM, Paterson I. Nat. Prod. Rep 2008;25:342. [PubMed: 18389141] (b) Paterson I, Florence GJ. Top. Curr. Chem 2009;286:73. (c) Smith AB III, Freeze BS. Tetrahedron 2008;39:261.
14. Mickel SJ, Niederer D, Daeffler R, Osmani A, Kuesters E, Schmid E, Schaer K, Gamboni R, Chen W, Loeser E, Kinder FR, Konigsberger K, Prasad K, Ramsey TM, Repic O, Wang R-M, Florence G, Lyothier I, Paterson I. Org. Process Res. Dev 2004;8:122.
15. (a) Mita A, Lockhart AC, Chen T-L, Bochinski K, Curtright J, Cooper W, Hammond L, Rothenberg M, Rowinsky E, Sharma S. J. Clin. Oncol 2004;22:2025. (b) Mita A, Lockhart A, Chen T. Proc. Am. Soc. Clin. Oncol 2004;23:133.
16. Snyder JP, Nettles JH, Cornett B, Downing KH, Nogales E. Proc. Natl. Acad. Sci. USA 2001;98:5312. [PubMed: 11309480]
17. Alcaraz AA, Mehta AK, Johnson SA, Snyder JP. J. Med. Chem 2006;49:2478. [PubMed: 16610791]
18. Geney R, Sun L, Pera P, Bernacki RJ, Xia S, Horwitz SB, Simmerling CL, Ojima I. Chem. Biol 2005;12:339. [PubMed: 15797218]
19. (a) Johnson SA, Alcaraz AA, Snyder JP. Org. Lett 2005;7:5549. [PubMed: 16320988] (b) Yang Y, Alcaraz AA, Snyder JP. J. Nat. Prod 2009;72:422. [PubMed: 19267457] (c) Sun L, Simmerling C, Ojima I. ChemMedChem 2009;4:719. [PubMed: 19360801]
20. Canales A, Matesanz R, Gardner NM, Andreu JM, Paterson I, Díaz JF, Jiménez-Barbero J. Chem. Eur. J 2008;14:7557.
21. (a) Monteagudo E, Cicero DO, Cornett B, Myles DC, Snyder JP. J. Am. Chem. Soc 2001;123:6929. [PubMed: 11448201] (b) Smith AB III, La Marche MJ, Falcone-Hindley M. Org. Lett 2001;3:695. [PubMed: 11259039] (c) Sánchez-Pedregal VM, Kubicek K, Meiler J, Lyothier I, Paterson I, Carlomagno T. Angew. Chem 2006;2006;118:7548.Angew. Chem. Int. Ed 45:7388.
22. Hoffmann RW. Angew. Chem 2000;2000;112:2134.Angew. Chem. Int. Ed 2000;39:2054.
23. Jogalekar AS, Kriel FH, Shi Q, Cornett B, Cicero D, Snyder JP. J. Med. Chem 2010;53:155. [PubMed: 19894728]
24. For dictyostatin analogues, see: (a) Shin Y, Choy N, Balachandran R, Madiraju C, Day BW, Curran DP. Org. Lett 2002;4:4443. [PubMed: 12465908] (b) Jung W-H, Harrison C, Shin Y, Fournier JH, Balachandran R, Raccor BS, Sikorski RP, Vogt A, Curran DP, Day BW. J. Med. Chem 2007;50:2951. [PubMed: 17542572] (c) Paterson I, Gardner NM, Poullennec KG, Wright AE. Bioorg. Med. Chem. Lett 2007;17:2443. [PubMed: 17336522] (d) Raccor BS, Vogt A, Sikorski RP, Madiraju C, Balanchandran R, Montgomery K, Shin Y, Fukui Y, Jung W-H, Curran DP, Day BW. Mol. Pharmacol 2008;73:718. [PubMed: 18073274] (e) Paterson I, Gardner NM, Poullennec KG, Wright AE. J. Nat. Prod 2008;71:364. [PubMed: 18081257] (f) Paterson I, Gardner NM, Guzman E, Wright E. Bioorg. Med. Chem. Lett 2008;18:6268. [PubMed: 18951787] (g) Eiseman JL, Bai L, Jung W-H, Moura-Letts G, Day BW, Curran DP. J. Med. Chem 2008;51:6650. [PubMed: 18839939] (h) Paterson I, Gardner NM, Naylor GJ. Pure Appl. Chem 2009;81:169. (i) Paterson I, Gardner NM, Guzman E, Wright AE. Bioorg. Med. Chem 2009:2282. [PubMed: 19022679] (j) Zhu W, Jiménez M, Jung W-H, Camarco DP, Balachandran R, Vogt A, Day BW, Curran DP. J. Am. Chem. Soc 2010;132:9175. [PubMed: 20545347]
25. For a preliminary account, see: Paterson I, Gardner NM. Chem. Commun 2007:49.
26. (a) Paterson I, Florence GJ, Gerlach K, Scott JP. Angew. Chem 2000;112:385.Angew. Chem. Int. Ed 2000;39:377. (b) Paterson I, Florence GJ, Gerlach K, Scott JP, Sereinig N. J. Am. Chem. Soc 2001;123:9535. [PubMed: 11572673] (c) Paterson I, Delgado O, Florence GJ, O'Brien M, Scott

JP, Sereinig N. J. Org. Chem 2005;70:150. [PubMed: 15624917] (d) Paterson I, Delgado O, Florence GJ, Lyothier I, Scott JP, Sereinig N. Org. Lett 2003;5:35. [PubMed: 12509884]

27. Inanaga J, Hirata K, Saeki H, Katsuki T, Yamaguchi M. Bull. Chem. Soc. Jpn 1979;52:1989.
28. Congreve MS, Davison EC, Fuhry MAM, Holmes AB, Payne AN, Robinson RA, Ward SE. Synlett 1993:663.
29. De Mico A, Margarita R, Parlanti L, Vescovi A, Piancatelli G. J. Org. Chem 1997;62:6974.
30. Still WC, Gennari C. Tetrahedron Lett 1983;24:4405.
31. Corey EJ, Bakshi RK, Shibata S. J. Am. Chem. Soc 1987;109:5551.
32. Paterson I, Britton R, Delgado O, Meyer A, Poullennec KG. Angew. Chem 2004;2004;116:4729.Angew. Chem. Int. Ed 2004;43:4629.
33. For a preliminary account, see: Paterson I, Naylor GJ, Wright AE. Chem. Commun 2008:4628.
34. Paterson I, Britton R, Delgado O, Gardner NM, Meyer A, Naylor GJ, Poullennec KG. Tetrahedron 2010;66:6534.
35. Evans DA, Chapman KT, Carreira EM. J. Am. Chem. Soc 1988;110:3560.
36. Allred GD, Liebeskind LS. J. Am. Chem. Soc 1996;118:2748.
37. Gunasekera SP, Longley RE, Isbruker RA. J. Nat. Prod 2002;65:1830. [PubMed: 12502323]
38. Mahoney WS, Brestensky DM, Stryker JM. J. Am. Chem. Soc 1988;110:291.
39. This rationalization was substantiated when an attempted reduction of the earlier β-hydroxy ketone with the enantiomeric (*S*)-CBS reagent failed to overturn the selectivity, continuing to generate the 1,3-*anti-diol* as the major diastereomer (4:1 dr).
40. This isomerism of the dienoate had also been observed in the synthesis of 10,11-dihydro dictyostatin **22**. A reversible 1,4-conjugate addition of DMAP being the most likely mechanism. Suitable conditions have since been developed to minimize this side-reaction, as reported in ref 34. For the Curran Group's approach to this problem, see ref 24j.
41. For a preliminary account, see: Paterson I, Naylor GJ, Fujita T, Guzmán E, Wright AE. Chem. Commun 2010;46:261.
42. (a) Ojima I, Habus I, Zhao M, Zucco M, Park YH, Sun CM, Brigaud T. Tetrahedron 1992;48:6985. (b) Ojima I, Sun CM, Zucco M, Park YH, Duclos O, Kuduk S. Tetrahedron Lett 1993;34:4149. (c) Holton RA. Eur. Pat. Appl. EP400 971 :971. (Chem. Abstr. 1991, 114, 164568q).
43. Prepared by adapting the method of Farina *et al*., see Farina V, Hauck SI, Walker DG. Synlett 1992:761.

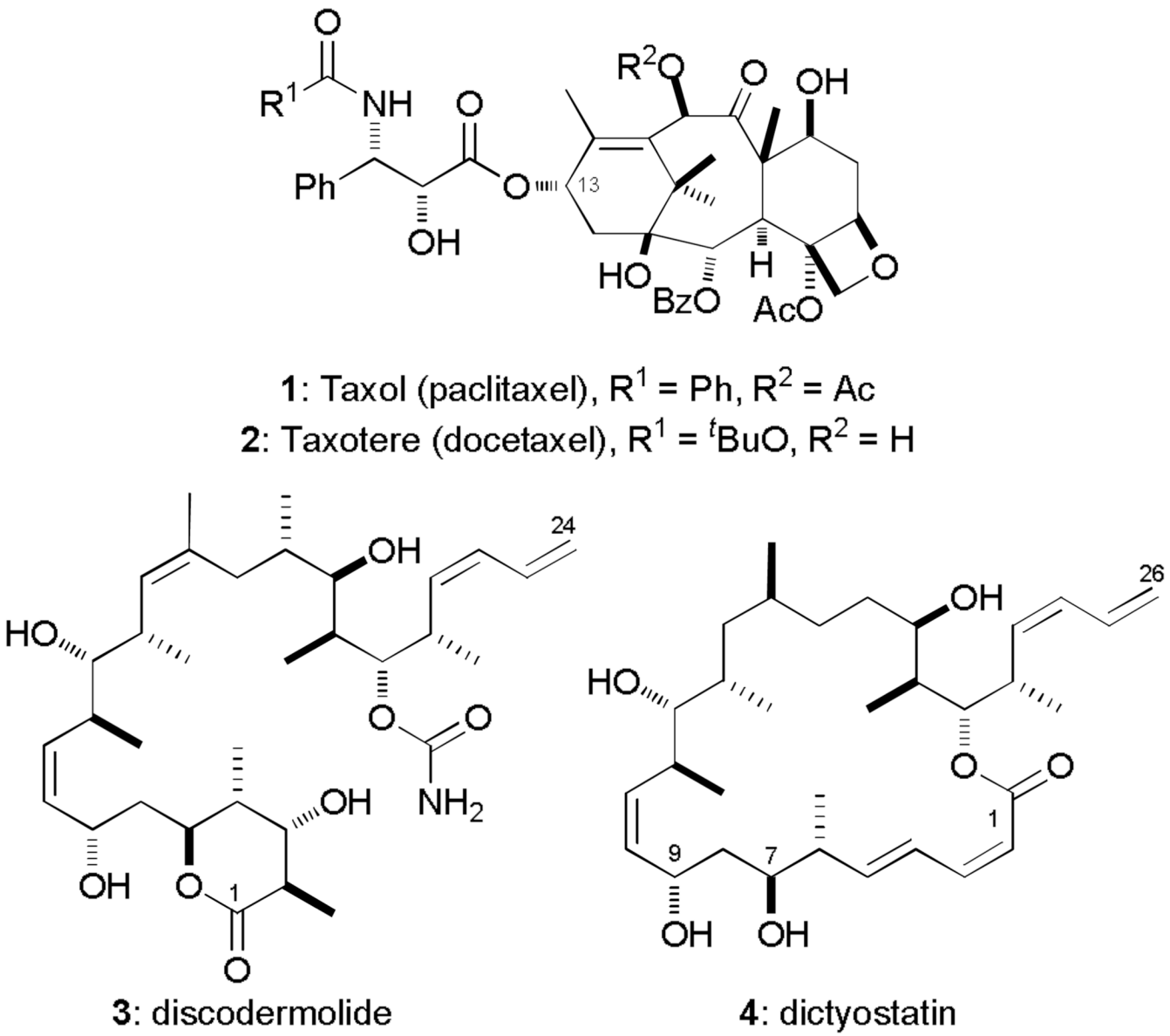

Figure 1.
Microtubule-stabilising agents Taxol (paclitaxel, **1**), Taxotere (docetaxel, **2**), discodermolide (**3**) and dictyostatin (**4**).

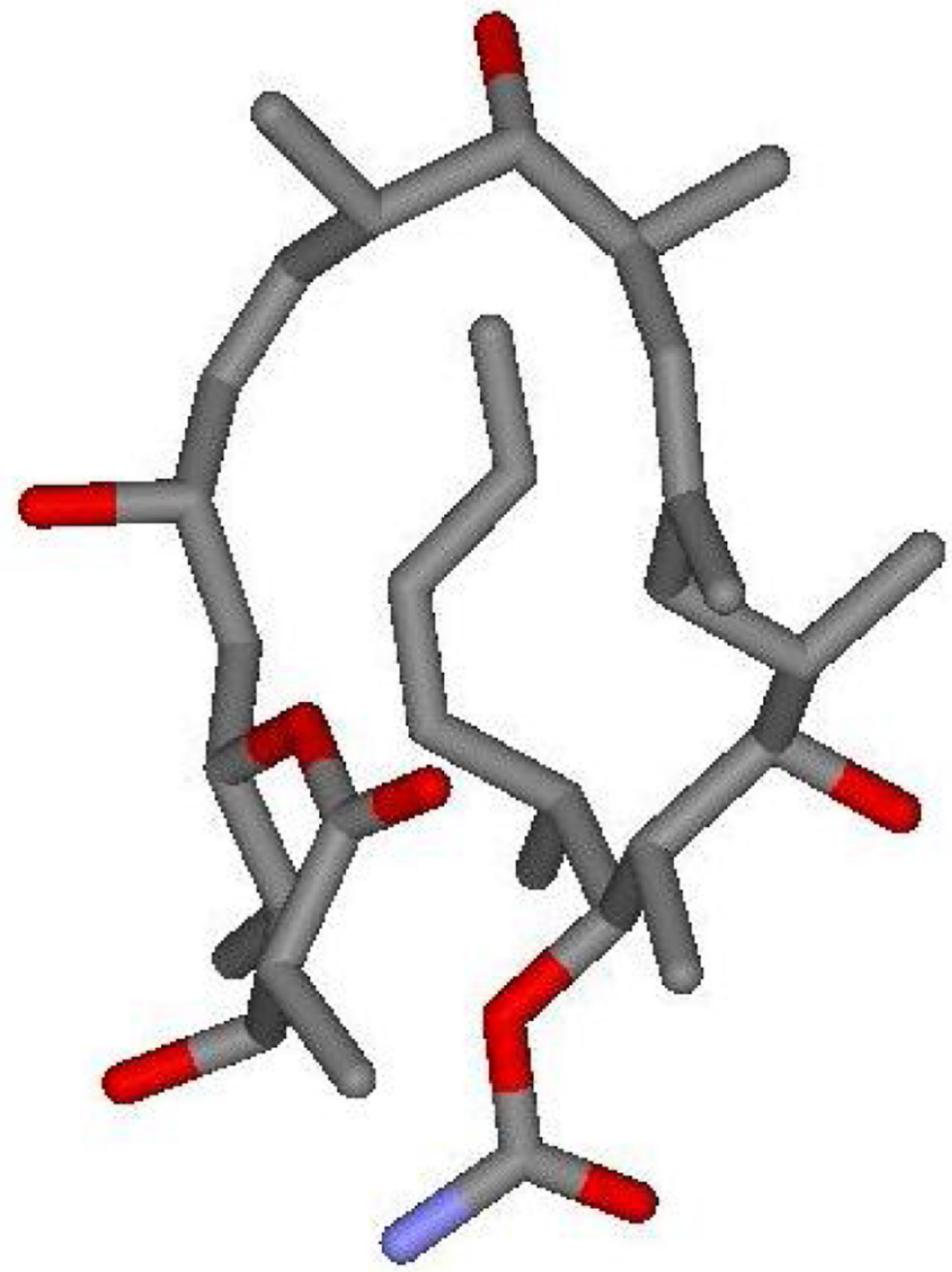

Figure 2.
The lowest energy conformer of discodermolide in D_2O as deduced by Canales *et al*[20] This hairpin conformation is broadly similar to the single-crystal X-ray structure of discodermolide in the solid state.

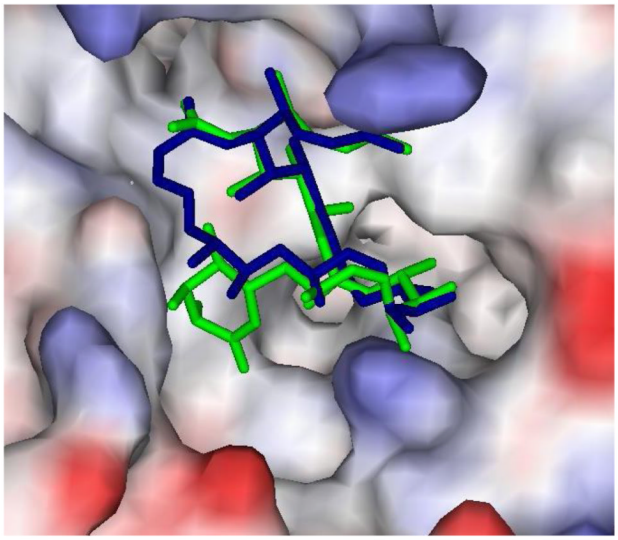

Image 1

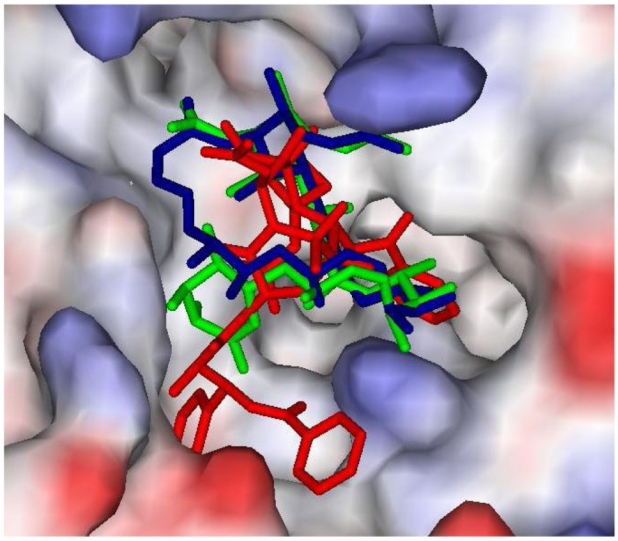

Image 2

Figure 3.
The microtubule-bound bioactive conformations of discodermolide (green) and dictyostatin (blue) overlaid at the taxoid binding site on β-tubulin, as calculated with AutoDock by Canales *et al*[20] (Image 1). In Image 2, taxol (red) has also been included, the additional region of the binding pocket exploited by the C13 ester side chain can be distinguished.

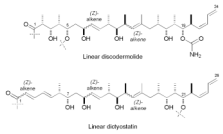

Figure 4.

Representations of C1–C24 and C1–C26 carbon chains of discodermolide (**3**) and dictyostatin (**4**) drawn in a linear manner to allow comparison of the matching stereochemistry and structural features.

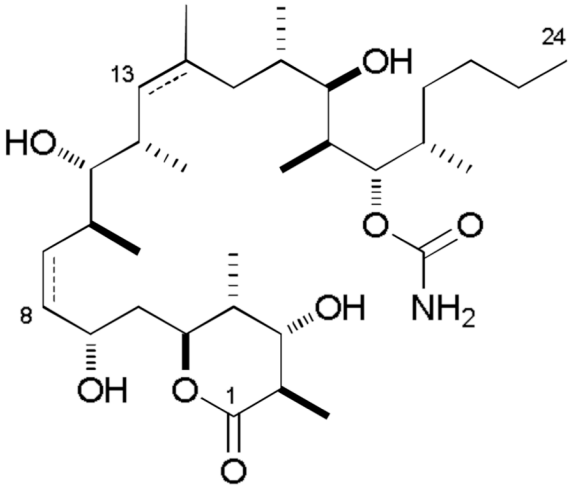

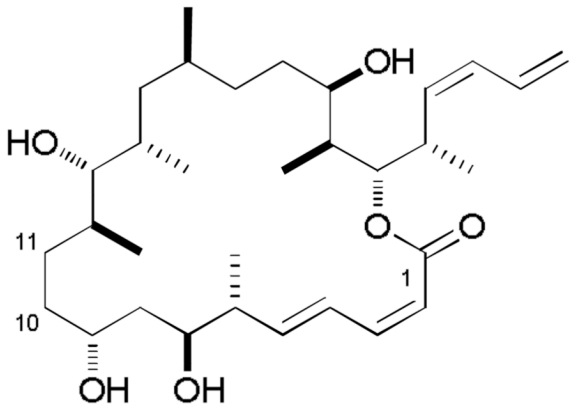

22: 10,11-dihydrodictyostatin

P-388, IC_{50} / nM	
19: fully saturated	>8292
20: $\Delta^{8,9}$, $\Delta^{13,14}$	10
21: $\Delta^{13,14}$	33.8

	IC_{50} / nM
AsPC-1	43
DLD-1	10
PANC-1	18
NCI/ADR	300

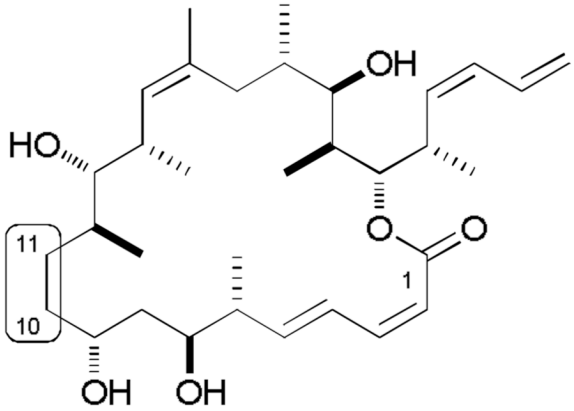

23

Figure 5.
Reduced derivatives of discodermolide with various levels of saturation (**19, 20** and **21**) and structures of 10,11-dihydro analogues **22** and **23** of dictyostatin and hybrid **12** respectively.

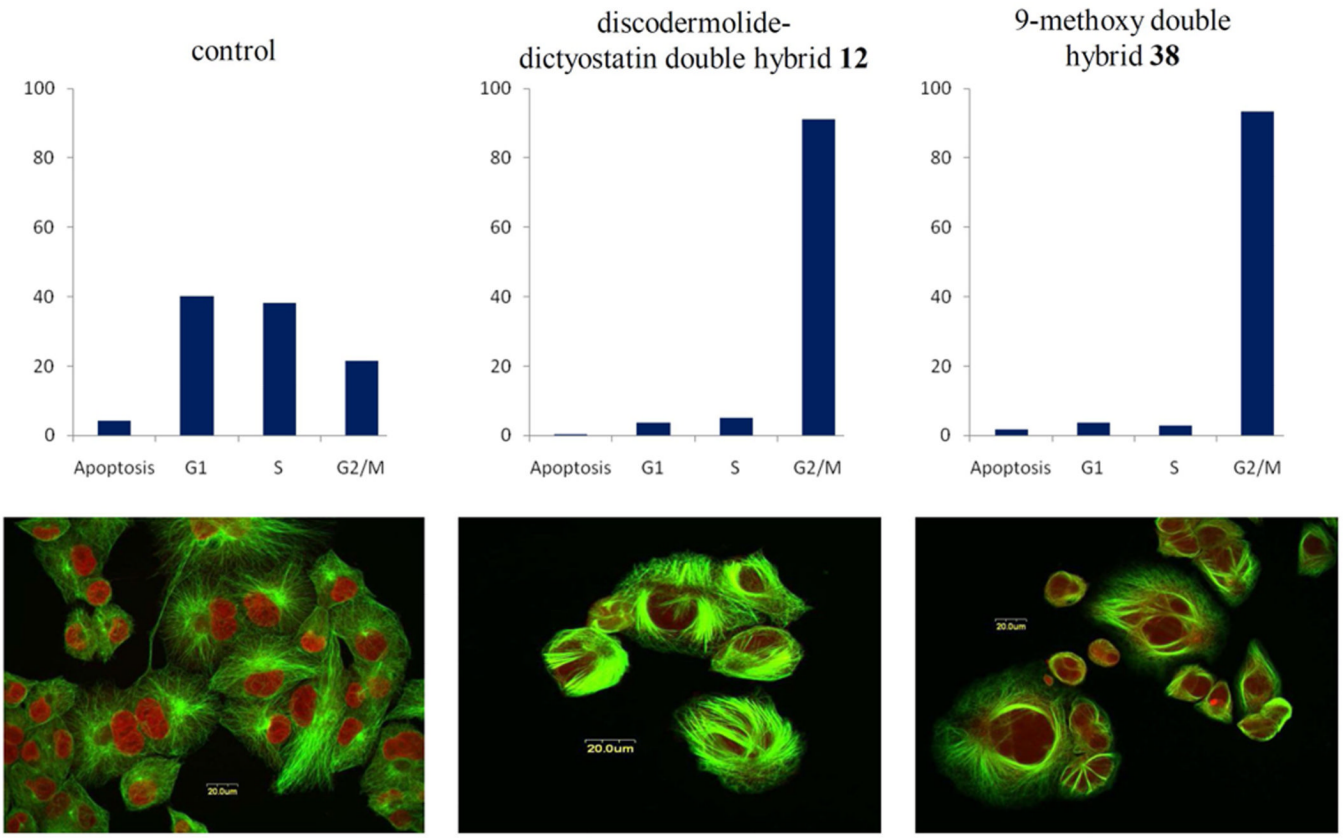

Figure 6.

(Graphs) Cell cycle analysis by flow cytometry of PANC-1 cells incubated for 24 h with DMSO (control), 100 nM dictyostatin/discodermolide hybrid **12** or 9-methoxy derivative **38**. Histograms represent samples of approximately 1×10^4 cells per test and are plotted as percentage (*y*-axis) vs stage of cell cycle (*x*-axis). Both compounds result in an accumulation of cells in the G2/M phase. (Images) Immunofluorescence images of PANC-1 cells stained with anti-α-tubulin (green) and propidium iodide (red) and observed with confocal microscopy. Cells were exposed to DMSO (control), 100 nM **12** or 100 nM **38**. Dense microtubule bundling can be seen around the nuclei on treatment with **12** and **38**, a characteristic feature of microtubule-stabilising agents.

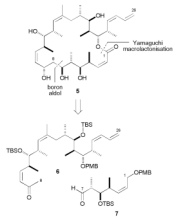

Scheme 1.
Retrosynthetic analysis of dictyostatin/discodermolide hybrid **5**.

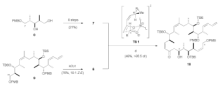

Scheme 2.

Generation of aldol adduct **10**. a) BCl_3·DMS, CH_2Cl_2, −78 → 0 °C, 2 h; b) TEMPO, $PhI(OAc)_2$, CH_2Cl_2, 20 °C, 2 h; c) K_2CO_3, 18-crown-6, methyl-*P*, *P*, *bis*-(2,2,2-trifluoroethyl)phosphonoacetate, PhMe / HMPA, 0 °C, 16 h; d) 1. **6**, Et_3N, *c*-Hex_2BCl, Et_2O, 0 °C, 1 h; **7**, −78 °C, 15 min; 2. pH 7 buffer (>95 : 5 dr, 48%). DMS = dimethyl sulfide; HMPA = hexamethylphosphoramide.

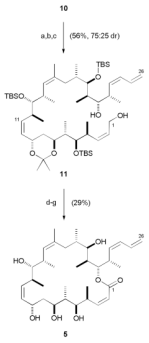

Scheme 3.

Completion of dictyostatin/discodermolide hybrid **5**. a) (*R*)-CBS, BH_3·THF, CH_2Cl_2, 0 °C, 3 h; b) cat. PPTS, $(MeO)_2CMe_2$, 20 °C, 2 h; c) DDQ, CH_2Cl_2 / pH 7 buffer, 20 °C, 3 h; d) cat. TEMPO, $PhI(OAc)_2$, CH_2Cl_2, 0 → 20 °C, 1 h; e) $NaClO_2$, NaH_2PO_4, 2-methyl-2-butene, ^tBuOH / H_2O, 20 °C, 4 h; f) 2,4,6-trichlorobenzoylchloride, Et_3N, PhMe, 20 °C, 40 min; DMAP, 20 °C, 20 min; g) 3N HCl, MeOH, 0 → 20 °C, 8 h. CBS = Corey-Bakshi-Shibata catalyst; PPTS = pyridinium *para*-toluenesulfonic acid; DDQ = 2,3-dichloro-5,6-dicyano-1,4-benzoquinone; TEMPO = 2,2,6,6-tetramethylpiperidine-1-oxy radical; DMAP = 4-dimethylaminopyridine.

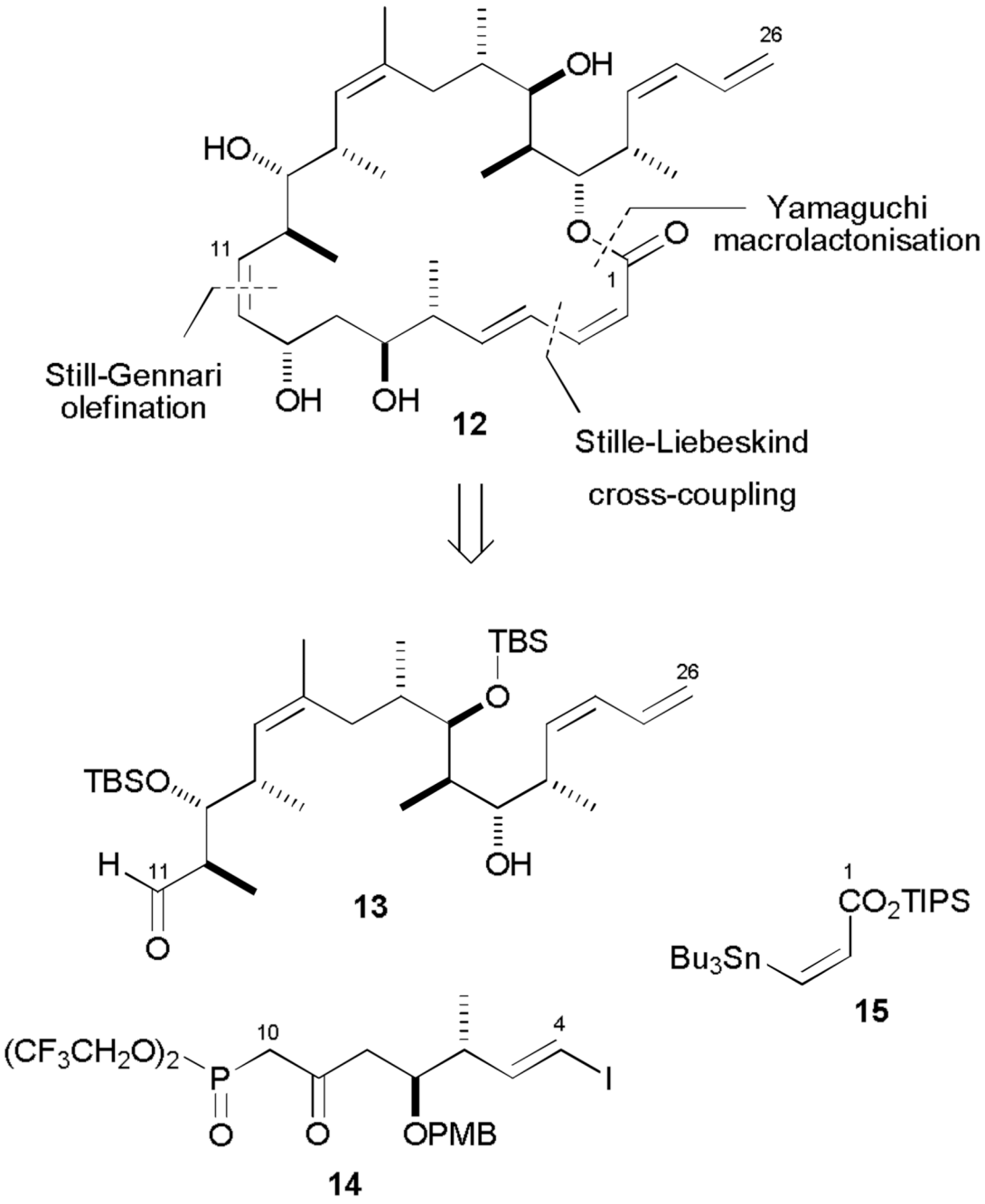

Scheme 4.
Retrosynthesis of dictyostatin/discodermolide hybrid **12**, leading to fragments **13, 14** and **15**.

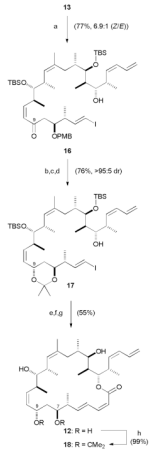

Scheme 5.

Endgame leading to dictyostatin/discodermolide hybrid **12** and acetonide **18**. a) **14**, K_2CO_3, 18-crown-6, PhMe / HMPA, 0 °C, 7 d; b) DDQ, CH_2Cl_2 / pH 7 buffer, 0 °C, 2.5 h; c) (*R*)-CBS, BH_3· THF, THF, −30 °C, 36 h; d) PPTS, $(MeO)_2CMe_2$, CH_2Cl_2, 0 → 20 °C, 16 h; e) 1. **15**, CuTC, NMP, 20 °C, 16 h; 2. KF, MeOH / THF, 20 °C, 90 min; f) 2,4,6-trichlorobenzoylchloride, Et_3N, PhMe, 20 °C, 1 h; DMAP, 20 °C, 4 d; g) 3N HCl, MeOH, 0 → 20 °C, 16 h; h) PPTS, $(MeO)_2CMe_2$, 0 → 20 °C, 16 h. CuTC = copper(I)-thiophene-2-carboxylate; NMP =*N*-methylpyrrolidinone.

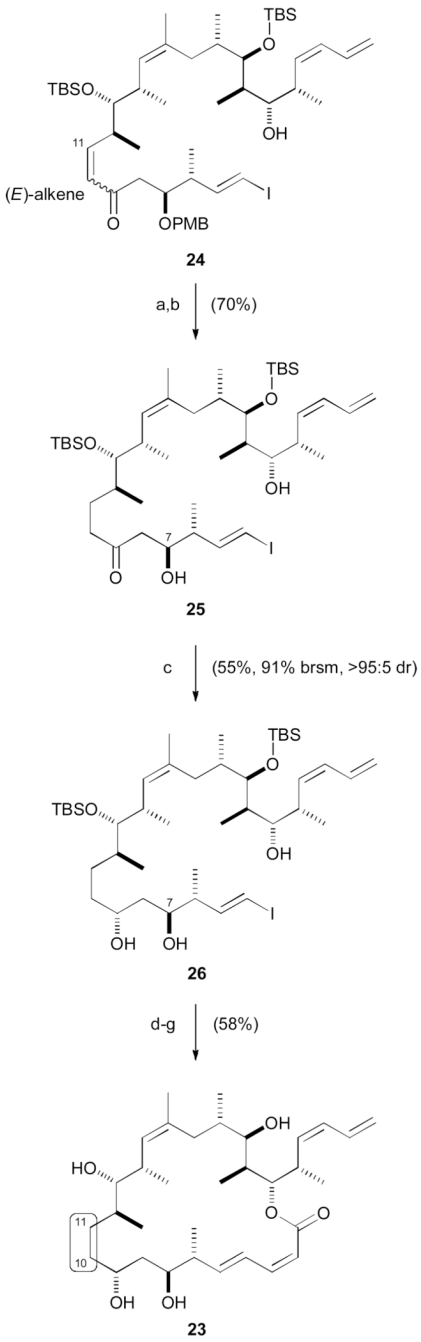

Scheme 6.

Completion of 10,11-dihydro dictyostatin/discodermolide hybrid **23**. a) $[PPh_3CuH]_6$, PhMe / H_2O, 20 °C, 16 h; b) DDQ, CH_2Cl_2 / pH 7 buffer, 0 °C, 2.5 h; c) $Me_4NBH(OAc)_3$, MeCN / THF, 0 °C, 16 h; d) PPTS, $(MeO)_2CMe_2$, CH_2Cl_2, 0 → 20 °C, 16 h; e) 1. **15**, CuTC, NMP, 20 °C, 16 h; 2. KF, MeOH / THF, 20 °C, 2 h; f) 2,4,6-trichlorobenzoylchloride, Et_3N, PhMe, 20 °C, 1 h; DMAP, 20 °C, 1 d; g) 3N HCl, MeOH, 0 → 20 °C, 16 h.

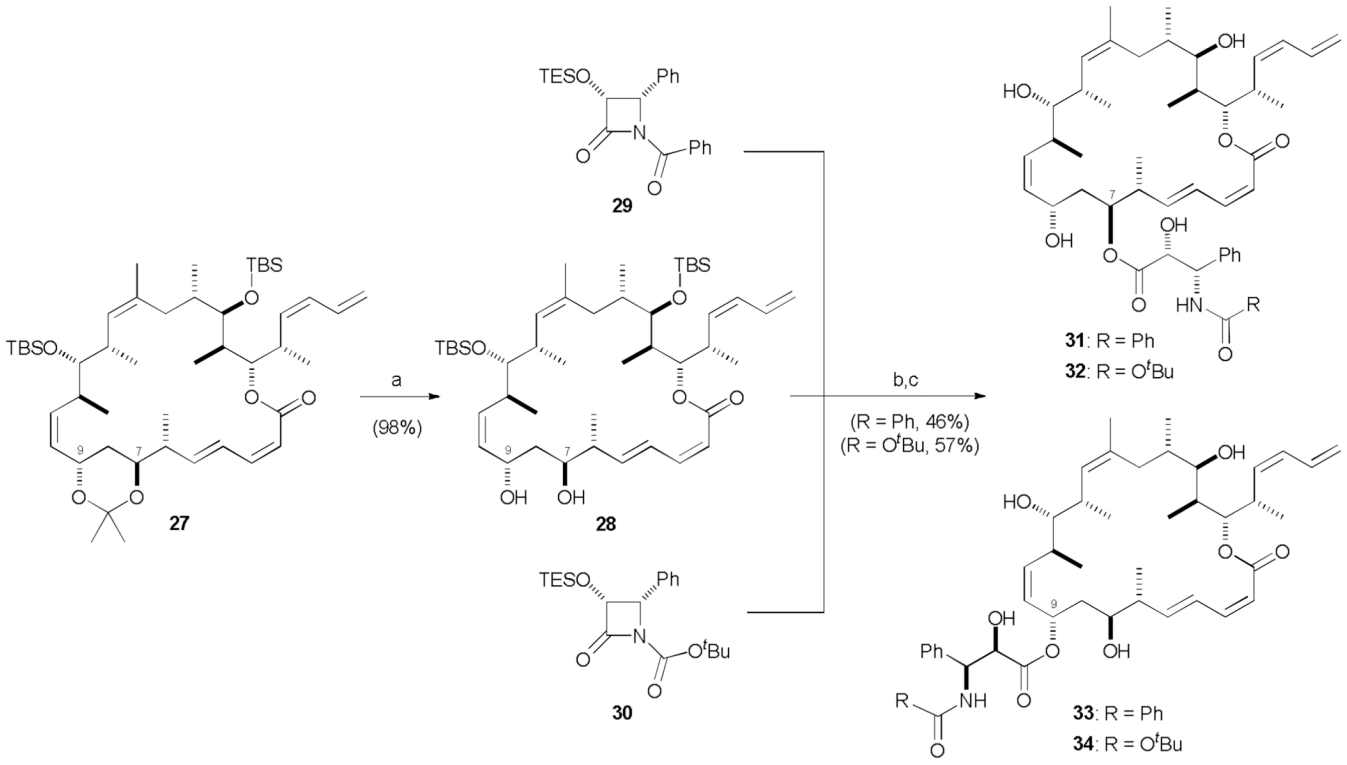

Scheme 7.

Generation of triple hybrids **31–34**. a) PPTS, MeOH / CH_2Cl_2, 0 → 20 °C, 16 h; b) NaHMDS, THF, −78 °C, 10 min; **29** or **30**, −78 → 0 °C, 30 min; c) HF·py, pyridine, THF, 0 → 20 °C, 3 d. NaHMDS = sodium hexamethyldisilazide.

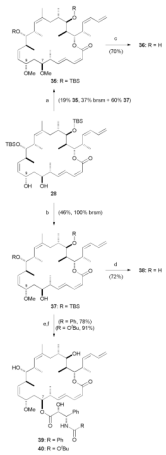

Scheme 8.

Synthesis of C9-methoxy analogues **36** and **38–40**. a) $Me_3O{\cdot}BF_4$, Proton Sponge, CH_2Cl_2, 20 °C, 70 min; b) $Me_3O{\cdot}BF_4$, Proton Sponge, CH_2Cl_2, 20 °C, 45 min; c) 3N HCl, MeOH, 0 → 20 °C, 16 h; d) HF·py, pyridine, THF, 0 → 20 °C, 3 d. e) NaHMDS, THF, −78 °C, 10 min; **29** or **30**, −78 → 0 °C, 30 min; f) HF·py, pyridine, THF, 0 → 20 °C, 3 d.

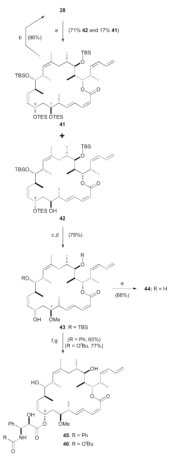

Scheme 9.

Completion of C7-methoxy analogues **44**–**46**. a) TESOTf, 2,6-lutidine, CH_2Cl_2, −98 °C, 90 min; b) PPTS, MeOH / CH_2Cl_2, 0 → 20 °C, 2 h; c) $Me_3O{\cdot}BF_4$, Proton Sponge, CH_2Cl_2, 20 °C, 90 min; d) PPTS, MeOH / CH_2Cl_2, 0 → 20 °C, 2 h; e) HF·py, pyridine, THF, 0 → 20 °C, 3 d; f) NaHMDS, THF, −78 °C, 10 min; **29** or **30**, −78 → 0 °C; g) HF·py, pyridine, THF, 0 → 20 °C, 3 d. TESOTf = triethylsilyl trifluoromethanesulfonate.

Table 1

Cytotoxicity of taxol (**1**), discodermolide (**3**), dictyostatin (**4**) and all prepared analogues and hybrids in cultured human cancer cell lines.

Compound	IC_{50}/nM			
	PANC-1 (pancreatic)	**NCI/ADR-Res (Taxol-resistant)**	**AsPC-1 (pancreatic)**	**DLD-1 (colon)**
Taxol (**1**)	9.9 ± 1.3	1264 ± 141	149 ± 33	22 ± 1
Discodermolide (**3**)	59 ± 34	160 ± 34	98 ± 34	29 ± 8
Dictyostatin (**4**)	4.2 ± 0.5	6.6 ± 0.4	6.2 ± 0.6	2.2 ± 0.5
Double hybrid **5**	1800	8200	2800	2100
Double hybrid **12**	12 ± 2.0	66 ± 15	34 ± 6.4	6.0 ± 1.1
Double hybrid **23**	138 ± 34	1450 ± 140	781 ± 100	130 ± 13
Acetonide **18**	4860 ± 150	2930 ± 300	4830 ± 450	2350 ± 180
Triple hybrid **31**	316 ± 56	4880 ± 420	–	–
Triple hybrid **32**	181 ± 37	3090 ± 500	–	–
Triple hybrid **33**	212 ± 45	2360 ± 100	–	–
Triple hybrid **34**	224 ± 8.0	3250 ± 300	–	–
Double hybrid **38**	17 ± 6.6	8.2 ± 4.3	–	–
Double hybrid **44**	47 ± 2.8	380 ± 47	–	–
Double hybrid **36**	60 ± 12	128 ± 11	–	–
Triple hybrid **39**	293 ± 40	974 ± 14	–	–
Triple hybrid **40**	190 ± 14	2040 ± 630	–	–
Triple hybrid **45**	460 ± 50	2540 ± 450	–	–
Triple hybrid **46**	412 ± 118	4400 ± 670	–	–